

Running head: Coordination of proline, lipid and redox metabolism

Corresponding Author:

Paul E. Verslues

Institute of Plant and Microbial Biology

Academia Sinica

No. 128 Sec. 2 Academia Rd, Nankang Dist.

Taipei, 11529

Taiwan

Phone: 886-2-2787-1186

FAX: 886-2-2782-7954

Email: paulv@gate.sinica.edu.tw

Proline coordination with fatty acid synthesis and redox metabolism of chloroplast and mitochondria¹

Suhas Shinde², Joji Grace Villamor³, Wendar Lin, Sandeep Sharma⁴, Paul E. Verslues⁵

Institute of Plant and Microbial Biology, Academia Sinica, Taipei 115, Taiwan

One sentence summary: A *Proline Dehydrogenase1 promoter:luciferase* screen and transcriptome of the proline synthesis mutant *p5cs1-4* find coordination between proline and multiple redox-related metabolic pathways.

Author Contributions: S. Shinde analyzed mutants and transgenic plants, analyzed data, assisted in manuscript writing and performed all other experiments not attributed to other authors; J.G.V. constructed the promoter-reporter line and did preliminary experiments for the mutant screen; W.L. analyzed mRNA sequencing data and SNP data for mapping; S. Sharma prepared samples for RNA sequencing and analyzed data; P.E.V. conceived and planned research, analyzed data, and prepared the manuscript with assistance from S. Shinde.

Footnotes:

1. This work was supported the Taiwan Ministry of Science and Technology (NSC 102-2628-B-001-003 to P.E.V.) and by an Academia Sinica Career Development Award to P.E.V.
2. Present Address: Department of Biological Sciences, East Tennessee State University, Johnson City, TN 37614
3. Present Address: Protease Degradomics Group, Central Institute for Engineering, Electronics and Analytics Forschungszentrum Jülich, 52425 Jülich, Germany
4. Present Address: Marine Biotechnology and Ecology Division, CSIR-Central Salt and Marine Chemicals Research Institute, Bhavnagar, Gujarat, India
5. Corresponding author email: paulv@gate.sinica.edu.tw

Abstract

Proline accumulation is one of the most prominent changes in plant metabolism during drought and low water potential; however, regulation and function of proline metabolism remain unclear. We used a combination of forward genetic screening based on a *Proline Dehydrogenase1* (*PDH1*) promoter-luciferase reporter (*PDH1_{pro}:LUC2*) and RNA sequencing of the proline synthesis mutant *p5cs1-4* to identify multiple loci affecting proline accumulation. Two mutants having high *PDH1_{pro}:LUC2* expression and increased proline accumulation at low water potential were found to be alleles of Cytochrome P450, Family 86, Subfamily A, Polypeptide 2 (*CYP86A2*) and Long Chain Acyl Synthetase2 (*LACS2*), which catalyze two successive steps in Very-Long Chain Fatty Acid (VLCFA) synthesis. Reverse genetic experiments found additional VLCFA and lipid metabolism-related mutants with increased proline accumulation. Altered cellular redox status is a key factor in coordination of proline and VLCFA metabolism. The NADPH-oxidase inhibitor diphenyleneiodonium (DPI) induced high levels of proline accumulation and strongly repressed *PDH1_{pro}:LUC2* expression. *cyp86a2* and *lacs2* mutants were hypersensitive to DPI but could be reverted to wild type proline and *PDH1_{pro}:LUC2* expression by ROS scavengers. Coordination of proline and redox metabolism was also indicated by altered expression of chloroplast and mitochondria electron transport genes in *p5cs1-4*. The results show that proline metabolism is both influenced by and influences cellular redox status via previously unknown coordination with several metabolic pathways. In particular, proline and VLCFA synthesis share dual roles to help buffer cellular redox status while producing products useful for stress resistance, namely the compatible solute proline and cuticle lipids.

Proline accumulation occurs in many plant species and can be induced by several types of abiotic stresses including drought (Szabados and Savoure, 2010; Verslues and Sharma, 2010). Altered proline metabolism can also have effects on plant development (Funck et al., 2012; Mattioli et al., 2012; Kavi Kishor et al., 2015). Of the many stimuli that can influence proline, it is drought and low water potential (ψ_w) that induce the highest levels of proline accumulation. There has been considerable effort to modify proline metabolism to enhance drought resistance (see for example Zhu et al., 1998; Nanjo et al., 1999; Roosens et al., 2002; Sawahel and Hassan, 2002; de Ronde et al., 2004; Su and Wu, 2004; Gleeson et al., 2005). Such efforts have been impeded by unresolved questions of why plants accumulate proline and how it contributes to drought tolerance. Substantial evidence indicates a role for proline in osmotic adjustment based both on the high levels of proline accumulation and observations that it predominantly accumulates in the relatively small volume of the cytoplasm and organelles (Voetberg and Sharp, 1991; Bussis and Heineke, 1998). However, osmotic adjustment is not the only role of proline accumulation. More recent data has emphasized the connection of proline to redox status (Sharma et al., 2011; Ben Rejeb et al., 2014; Ben Rejeb et al., 2015) and demonstrated that both proline synthesis and catabolism are essential to promote drought tolerance (Sharma et al., 2011; Bhaskara et al., 2015). The overall picture that emerges is that both the level of proline accumulated as well as the turnover of proline and its connection to broader metabolic status must be considered to fully understand the role of proline metabolism in drought resistance (Szabados and Savoure, 2010; Bhaskara et al., 2015).

Proline is synthesized by conversion of glutamate to the intermediate Δ^1 -pyrroline-5-carboxylate (P5C) by P5C synthetase (P5CS) and P5C is then converted to proline by P5C reductase (P5CR) (Szabados and Savoure, 2010; Verslues and Sharma, 2010). P5CS utilizes NADPH as a cofactor (Zhang et al., 1995). P5CR can utilize both NADH and NADPH; however, recent work indicates that NADPH is the predominant source of reductant used by P5CR *in vivo* (Giberti et al., 2014). Arabidopsis has two *P5CS* genes which are not functionally equivalent (Szekely et al., 2008). *P5CS1* is induced by drought and related stresses at both the transcript and protein levels and is thought to be the rate limiting step for stress-induced proline synthesis. *p5cs1* mutants have greatly reduced proline accumulation during low ψ_w or salt stress but have normal growth and morphology under unstressed conditions (Szekely et al., 2008;

Sharma et al., 2011; Bhaskara et al., 2015). Despite many stress-related studies which have measured or manipulated *P5CS1* gene expression, how P5CS1-mediated proline synthesis is regulated and interacts with other metabolic pathways is still unclear.

Proline catabolism occurs in the mitochondria via proline dehydrogenase (PDH) which converts proline to P5C and P5C Dehydrogenase (P5CDH) which converts P5C back to glutamate; thus forming the proline cycle (Szabados and Savoure, 2010; Verslues and Sharma, 2010). A unique feature of PDH is that it donates electrons directly to the mitochondrial electron transport chain; however, mechanistic details and identity of the electron acceptor are not firmly established in plants (Szabados and Savoure, 2010; Verslues and Sharma, 2010). Of the two *Arabidopsis* genes which encode PDH, *PDH1* is more highly expressed and is thought to have a predominant role in proline catabolism (Funck et al., 2010). *PDH1* expression is down regulated by drought stress in much of the plant (Peng et al., 1996; Yoshida et al., 1997; Sharma and Verslues, 2010). Conversely, *PDH1* is induced by exogenous proline and this induction involves a cis-element containing the sequence ACTCAT, referred to as the Proline Response Element (ProRE; Satoh et al., 2002). The ProRE is bound by several bZIP transcription factors which can upregulate *PDH1* in response to exogenous proline, starvation and perhaps other signals (Satoh et al., 2004; Weltmeier et al., 2006; Dietrich et al., 2011). The upstream factors that regulate activity of these bZIPs are not known. The up-regulation of *PDH1* in response to proline presents an unresolved paradox. During drought stress a high level of proline accumulates; yet, rather than be induced by this high level of proline, *PDH1* is down-regulated in most plant tissues (Miller et al., 2005). Thus *PDH1* is regulated by incompletely understood mechanisms that likely reflect both stress and metabolic signals. All these factors make *PDH1* an excellent marker to study the intersection of stress signaling and metabolic regulation.

We used a forward genetic screen based on expression of a *PDH1 promoter:Luciferase* construct combined with mapping-by-sequencing to identify factors affecting *PDH1* expression and proline accumulation. This screen found an unexpected effect of Very Long Chain Fatty Acid (VLCFA) synthesis on proline accumulation. Several lines of evidence indicate that reduced VLCFA synthesis affects proline accumulation via effects on redox status rather than signaling functions of VLCFA metabolism enzymes or lipid metabolism intermediates. In parallel, mRNA sequencing of *p5cs1-4*, which has reduced proline synthesis, found substantial

effects on chloroplast and mitochondria gene expression consistent with a connection of proline to redox metabolism in both organelles. Together, these results show the extensive coordination of proline metabolism with multiple metabolic pathways related to cellular redox status.

Results

A mutant screen based on the *PDHI* promoter identifies mutants of *CYP86A2* and *LACS2* with increased proline accumulation at low ψ_w

A forward genetic screen was developed to identify factors affecting *PDHI* expression and proline accumulation. A 1.5 kb fragment of the *PDHI* promoter and 5' UTR was used to drive expression of the Luciferase2 reporter (*PDHI_{pro}:LUC2*). Several *Arabidopsis thaliana* (Col-0 accession) transgenic lines containing single locus insertions of the *PDHI_{pro}:LUC2* reporter were isolated. A single line having five-fold down regulation of *PDHI_{pro}:LUC2* in response to low ψ_w , essentially identical to the endogenous *PDHI* [Fig. 1; Sharma and Verslues (2010)], was selected for further study. This un-mutagenized *PDHI_{pro}:LUC2* line is referred to as “wild type” (W.T.) in subsequent figures. After ethyl methanesulfonate (EMS) mutagenesis, screening in the M₁ and M₂ generations (Fig. S1) identified mutants with high or low *PDHI_{pro}:LUC2* expression. Candidate genes for a number of high *PDHI_{pro}:LUC2* mutants were identified using a mapping by sequencing approach and two such mutants are reported here.

Mutants 4442-4 and 4255-1 were phenotypically similar with each one having 3-fold increased *PDHI_{pro}:LUC2* expression in both control and stress treatments (Fig. 2A and B). Low ψ_w could still repress the expression of *PDHI_{pro}:LUC2* in 4442-4 and 4255-1 but not to the level seen in wild type. Also, both mutants had proline accumulation nearly twice that of wild type at -1.2 MPa (Fig. 2C) but did not differ from wild type in proline content of unstressed plants. Expression of the endogenous *PDHI* was increased approximately 3-fold in 4442-4 under unstressed conditions (Fig. 2D) and agreed well with the increased *PDHI_{pro}:LUC2* expression. However, at low ψ_w *PDHI* expression decreased to similar level as wild type despite the higher *PDHI_{pro}:LUC2* expression (Fig. 2D). Similar difference between *PDHI_{pro}:LUC2* expression and endogenous *PDHI* at low ψ_w was also observed in other high proline, high *PDHI_{pro}:LUC2* mutants in our collection (S. Mukuri, S. Shinde, P.E. Verslues, unpublished observations).

For 4442-4, sequencing of bulked segregants and Next Generation Mapping (Austin et al., 2011) identified several candidate genes (Fig. S2A). However, only mutants of Cytochrome P450, Family 86, Subfamily A, Polypeptide 2 (*cyp86a2*, *at4g00360*) had elevated proline levels similar to 4442-4 (Fig. 3A). Mutants of the two other candidate genes did not differ from wild type in proline accumulation (Fig. S2B). For 4255-1, *Long Chain Acyl-CoA Synthetase2* (*Atlg49430*) was identified as the main candidate gene (Fig. S2C) and *lacs2-1* (Schnurr et al., 2004) had increased proline accumulation similar to 4255-1 (Fig 3A). Genetic complementation found that F₁ seedlings of 4442-4 crossed to *cyp86a2-1* as well as 4255-1 crossed to *lacs2-1* had the same high *PDH1_{pro}:LUC2* expression as the homozygous mutant (Fig. 3B). This indicated that 4442-4 was an allele of *cyp86a2* and 4255-1 was an allele of *lacs2*.

Both LACS2 and CYP86A2 are ER-localized enzymes that catalyze successive steps in Very Long Chain Fatty Acid (VLCFA) synthesis: the esterification of C₁₆ and C₁₈ fatty acids to Co-Enzyme A and subsequent ω -hydroxylation of these fatty acids for synthesis of cutin monomers (Li-Beisson et al., 2013). EMS mutants 4442-4 and 4255-1 stained with toluidine blue (Fig. 3C) indicating that they share the previously reported cuticle defects of *cyp86a2* and *lacs2* (Xiao et al., 2004; Schnurr et al., 2004). We also transgenically complemented 4442-4 with *35S:CYP86A2* (Fig. 3C, Fig. 3D, Fig. 3E) and showed that introducing the *cyp86a2-1* and *lacs2-1* T-DNA mutants into the *PDH1_{pro}:LUC2* background produced the same high *PDH1_{pro}:LUC2* expression phenotype as the 4442-4 and 4255-1 EMS mutants (Fig. S3). 4442-4 has a point mutation that changes Gly37 to Asp (G to A transition at position 110 of the *CYP86A2* CDS). This mutation lies in the catalytic domain (amino acid 5-511 based on NCBI's conserved domain database [CDD] search) consistent with 4442-4 being a null allele of CYP86A2. For 4255-1, the mutation was in a cryptic splice site at the *LACS2* intron 10-exon 11 junction (G to A transition at position 18293272 of chromosome 1). Primers spanning intron 10 amplified a larger fragment in 4255-1 than in wild type (Fig. 3F) consistent with retention of the 84 bp intron 10. This alters the downstream reading frame thus preventing translation of functional LACS2 protein.

Further characterization of 4442-4 and 4255-1 as well as *cyp86a2-1* and *lacs2-1* T-DNA mutants found that the protein abundance and apparent molecular weight of PDH1 and P5CS1 were not altered in any of the mutants under either stress or control conditions (Fig. 4A). Thus,

cyp86a2 and *lacs2* did not affect post-translational regulation (for example redox-related post-translational modifications, see below) of these two key enzymes of proline metabolism. *P5CS1* gene expression, as well as expression of other proline metabolism genes, was also not substantially altered in *cyp86a2* mutants (Fig. S4). Further experiments with *cyp86a2* mutants found that they had increased proline across a range of low ψ_w severities with even a mild stress of -0.5 MPa leading to twice as much proline accumulation in *cyp86a2* as in wild type (Fig 4B). Interestingly, *cyp86a2* had the same proline accumulation as wild type in response to salt stress or exogenous ABA (Fig. 4B). Thus the effect of disrupting VLCFA synthesis on proline was specific to low ψ_w and occurred via an unknown mechanism which did not involve altered gene expression or modification of the two key proline metabolism enzymes P5CS1 and PDH1.

Additional mutants affecting VLCFA synthesis or cuticle deposition also have increased proline accumulation

The fact that both *CYP86A2* and *LACS2* were identified in our mutant screen suggested that the high proline accumulation and increased *PDH1_{pro}:LUC2* expression may not be due to a specific signaling or enzymatic function of the CYP86A2 or LACS2 proteins. As VLCFAs have been shown to have signaling function in controlling development (Nobusawa et al., 2013), there were several possible ways in which VLCFA metabolism could influence proline accumulation and *PDH1_{pro}:LUC2* expression. We hypothesized that either reduced flux through VLCFA synthesis, reduced levels of a product downstream of CYP86A2 or, increased levels of a lipid species upstream of LACS2 could cause the proline-related phenotypes of *cyp86a2* and *lacs2* mutants. As one way to test these possibilities, we isolated T-DNA mutants of other genes involved in VLCFA metabolism or its regulation. Of these, a mutant of *BODYGUARD* (*BDG*)/9-cis epoxycarotenoid defective1(*CED1*), a cuticle lipid transporter previously found to affect abiotic stress response (Wang et al., 2011b), had increased proline accumulation similar to *cyp86a2* and *lacs2-1* (Fig. 4C). Because CED1 functions downstream of *cyp86a2* and *lacs2*, these data indicated that it was not a reduced level of a lipid intermediate downstream of CYP86A2 that increased proline accumulation. Rather the blockage of VLCFA metabolism itself seemed a more likely cause. Consistent with this hypothesis, mutants of other VLCFA-related genes had moderate, but significant, increases in proline accumulation (Fig. 4C), likely reflecting the extent that VLCFA synthesis was disrupted. *CYP86A4* and *CYP77A6* are most

active in flowers with lesser effect on leaf cuticle (Li-Beisson et al., 2009) and had moderately increased or unaffected proline accumulation (Fig. 4C). Similarly, MYB16 and MYB106 have overlapping function such that each single mutant causes only partial blockage of flux through VLCFA synthesis (Oshima et al., 2013) and thus only moderate effect on proline accumulation. Other mutants or inhibitor treatments affecting lipid metabolism upstream of LACS2 also had high proline levels (see below), further indicating that reduced metabolic flux through lipid metabolism was the most likely cause of increased proline accumulation in *cyp86a2* and *lacs2-1*.

Cellular redox status is a factor in coordinating proline and VLCFA metabolism

Proline and VLCFA synthesis lead to different products and occur in different cellular compartments. However, a commonality is that both proline and VLCFA synthesis consume NADPH and regenerate NADP⁺ (Sharma et al., 2011; Li-Beisson et al., 2013; Giberti et al., 2014; Ben Rejeb et al., 2015) and thus can influence cellular redox status. To determine whether altered redox status was involved in the high proline and high *PDHI_{pro}:LUC2* expression of *cyp86a2* and *lacs2*, dithiothreitol (DTT) was used to increase reductant load while the ROS scavengers Ascorbic Acid (AsA) and *N,N'*-dimethylthiourea (DMTU) or the NADPH oxidase inhibitor diphenyleneiodonium (DPI) were used to decrease reductant load and interfere with ROS signaling. Treatment of unstressed Col-0 (wild type) with 5 or 20 mM DTT increased proline accumulation 4-fold and 30-fold, respectively (Fig. 5A). This was in agreement with previous results (Kolbe et al., 2006). *cyp86a2-1* and *lacs2-1* had greater response of proline accumulation to DTT (Fig. 5A). This was consistent with these mutants having altered redox status or less capacity to buffer redox status. Proline accumulation of *pdh1-2* was also more responsive to DTT while *p5cs1-4* was less responsive indicating that both proline synthesis and proline catabolism were involved in the response to DTT (Fig. 5A). We also observed that 20 mM, but not 5 mM, DTT increased proline accumulation at low ψ_w (Fig. 5B). Note that we did not analyze proline in mutants treated with 20 mM DTT or mutants treated with a combination of DTT and low ψ_w because the mutants were more sensitive to these treatments and exhibited bleaching and seedling death. Conversely, the ROS scavengers AsA and DMTU suppressed low ψ_w -induced proline accumulation of *cyp86a2-1* and *lacs2-1* back to the wild type level (Fig. 5C). AsA and DMTU also significantly inhibited the increased *PDHI_{pro}:LUC2* expression of 4442-4

and 4255-1 at low ψ_w (Fig 5D, F). DMTU also blocked the increased *PDH1_{pro}:LUC2* expression of unstressed 4442-4 and 4255-1 (Fig. 5E).

Also consistent with a role of redox or ROS in proline regulation, blocking NADPH oxidase activity using the inhibitor diphenyleneiodonium (DPI) caused a nearly 30-fold increase in proline content of Col-0 seedlings at high ψ_w (Fig. 6A). DPI treatment of unstressed W.T. seedlings (-0.25 MPa) completely suppressed *PDH1_{pro}:LUC2* expression to the level typically seen at low ψ_w (Fig. 6B). An even greater response to DPI was seen in *cyp86a2-1*, *lacs2-1* and *pdh1-2* as proline content increased 50 to 60-fold over the untreated control and *PDH1_{pro}:LUC2* activity was suppressed to the W.T. level (Fig. 6A, Fig 6B, -0.25 MPa data). Conversely, the response to DPI was less in *p5cs1-4*, indicating that proline synthesis via P5CS1 was required for DPI-induced proline accumulation. At low ψ_w , where proline levels are already high and *PDH1_{pro}:LUC2* expression lower, DPI had lesser effect (Fig. 6A and Fig. 6B).

Despite the DPI data, measurements of NADP⁺/NADPH found no significant differences between wild type and *cyp86a2* and *lacs2-1* (Fig. S5). There was an accumulation of NADPH in all genotypes at low ψ_w consistent with previous data (Sharma et al., 2011); however, we did not find significant difference in NADP⁺/NADPH ratio. We also did not see any differences in amount or localization of ROS staining between wild type, *cyp86a2-1* and *lacs2-1* (Fig. S6) indicating that uncontrolled ROS build up did not occur under our stress conditions. These assays do not rule out the involvement of NADP⁺/NADPH, increased ROS, or ROS signaling in the *cyp86a2* and *lacs2-1* phenotypes. However, when combined with the AsA, DMTU and DPI data, these measurements do suggest that any changes in ROS or pyridine nucleotide redox status may be specific to certain subcellular compartments. This is perhaps consistent with changes in VLCFA synthesis in the endoplasmic reticulum being communicated to proline metabolism in the cytoplasm and mitochondria by specific, but unknown, signaling mechanisms. In this way redox status may be buffered before damaging bulk changes in redox metabolites or ROS occur. Redox status of the chloroplast is also very likely to be involved in such redox communication and also may influence proline accumulation (see below)

RNA sequencing of *p5cs1-4* shows the influence of proline synthesis on redox metabolism of chloroplast and mitochondria

To further test the relationship between proline and redox-related metabolism, as well as more generally investigate the effects of reduced proline synthesis, mRNA sequencing of *p5cs1-4* was conducted. *p5cs1-4* lacks P5CS1 protein expression (Fig. 4A) and has greatly reduced proline accumulation and reduced growth at low ψ_w (Szekely et al., 2008; Sharma et al., 2011; Kesari et al., 2012; Bhaskara et al., 2015). For the Col-0 wild type, RNA sequencing (Table S1, Fig. 7A) found 1232 genes with significantly increased expression at low ψ_w with an enrichment of GO terms associated with abiotic stress (Table S2). Conversely, 1155 genes were down regulated (Table S3). As one way to access the quality of this data set, we compared it to microarray data from Bhaskara et al. (2012) who used the same 96 h, -1.2 MPa stress treatment. Approximately half the genes found to be stress up or down-regulated in Col-0 by RNA sequencing were also found to be up or down regulated in the microarray analysis of Bhaskara et al. (2012) (Fig. 7B). This is a substantial overlap between the two datasets when one considers that the RNA sequencing analysis detects genes not present on the ATH1 chips used by Bhaskara et al. (2012) and for high expression genes RNAseq can be more effective in detecting small changes in expression. Conversely, even large fold-change expression differences of genes with overall low expression (low read counts) did not pass the statistical cut-offs used in analyzing the RNAseq data.

For *p5cs1-4*, 111 genes were significantly up-regulated and 132 down-regulated compared to wild type Col-0 in the unstressed high ψ_w treatment. At low ψ_w 61 genes were significantly up-regulated and 106 genes down regulated in *p5cs1-4* compared to wild type Col-0 (Fig. 7B, Fig. 7D, Table S4-S7). There were three main patterns of interest in the *p5cs1-4* gene expression data. The most prominent pattern was that genes differentially expressed in *p5cs1-4* were strongly enriched for functions in chloroplast and mitochondrial redox metabolism (see significantly enriched GO categories in Tables S4-S7). This included a striking prevalence of chloroplast encoded genes among the genes having higher expression in unstressed *p5cs1-4* (14 chloroplast encoded genes out of 111 genes significantly upregulated (Table S4). The portion of chloroplast genes up-regulated in unstressed *p5cs1-4* was significantly higher (enriched) compared to the portion of chromosomal encoded genes (two tailed $p < 1 \times 10^{-16}$ by Fischer's

Exact Test). The genes upregulated in *p5cs1-4* at low ψ_w also had a significant enrichment of chloroplast encoded genes (7 out of 61 upregulated genes, Table S6; two tailed $p < 1 \times 10^{-8}$ by Fischer's Exact Test). In unstressed *p5cs1-4*, the majority of the most highly up-regulated genes (greater than 5-fold) were chloroplast encoded genes (Table S4). The effects of *p5cs1-4* on photosynthesis gene expression were concentrated in the light reactions while there was little effect of *p5cs1-4* on Calvin Cycle or photorespiration related genes (MapMan analysis, Fig. S7). In addition to these genes upregulated in *p5cs1-4*, GO analysis found strong and statistically significant enrichment of photosynthesis related functions among the genes downregulated in *p5cs1-4* (Tables S5 and S7).

Also striking was the observation that more than 30 genes encoding chloroplast or mitochondrial NAD(P)H Dehydrogenases, as well as genes involved in splicing or processing mitochondrial NAD genes, had higher RPKM values in *p5cs1-4* while only three such genes had lower RPKM in *p5cs1-4* (Table S10; note that this analysis included all genes with fold change more than two to include gene with large fold changes but which could not be called as significant changes because of low read counts in wild type). MapMan analysis also showed that *p5cs1-4* had a notably different expression pattern of genes encoding mitochondrial function genes, particularly genes in electron transport complex I, compared to wild type (Fig. S8). Also, *p5cs1-4* had altered expression of a number of other oxidation-reduction related genes of less clear function (such as *At5g11330*; Fig 7E). Together this data indicate substantially altered chloroplast and mitochondrial electron transport in *p5cs1-4* at both high and low ψ_w .

The second pattern of interest was the overall similar numbers of genes and similar GO enrichment profiles of up or down regulated genes in *p5cs1-4* for both control and stress treatments (Table S4-S7). There were differences in the individual genes significantly increased or decreased by *p5cs1-4* in control and stress treatments (Fig. 7D). This may be mainly a stochastic effect as a many genes narrowly missed our statistical cutoff in either the control or stress treatment. The genes up or down regulated in *p5cs1-4* included both genes whose expression was affected by stress in wild type and further altered in *p5cs1-4* as well as genes with altered expression in *p5cs1-4* but not affected by low ψ_w in wild type (Table S8-S9).

The third pattern of interest was the relative absence of amino acid and nitrogen metabolism functions among genes differentially expressed in *p5cs1-4*. The most strongly enriched GO terms in *p5cs1-4* up or down-regulated genes did not include any terms related to amino acid or nitrogen metabolism (Tables S4-S7; GO terms with $P \leq 0.001$). Only a few GO terms related to glutamate metabolism, ammonia transport or ammonia assimilation were found and these were overall less highly enriched (Tables S4-S7) and the number of genes represented in these categories was dwarfed by the number of genes in other functional categories. Even when all the genes with 2-fold or greater RPKM difference between *p5cs1-4* and wild type were included, MapMan analysis showed that very few genes mapped to amino acid and nitrogen metabolism pathways compared to greater numbers of genes in chloroplast light reactions and mitochondrial electron transport (Fig. S9). These observations are consistent with the conclusions of Less and Galili (2008) who found that transcriptional regulation of proline metabolism differed from that of other amino acid metabolism pathways. Thus, the *p5cs1-4* transcriptome analysis, as well as the *cyp86a2* and *lacs2* mutant experiments described above, indicated that proline metabolism is extensively coordinated with cellular redox status. This included chloroplast and mitochondrial electron transport as well as lipid metabolism. At the same time, the data indicated much less connection of proline to other aspects of carbon-nitrogen metabolism.

We also used the “Signature” tool in Genevestigator to find publically available microarray data with similar patterns of differentially expressed genes as *p5cs1-4* under either control or stress conditions. For *p5cs1-4* in the unstressed control treatment, this analysis found several data sets related to light signaling (*phyA* and *cop1* mutants) or different light treatments as well as salicylic acid (SA) treatment (Fig. S10). For *p5cs1-4* at low ψ_w there was similarity to gene expression changes observed in SA synthesis and signaling mutants (for example *sid2-1*, *npr1* and *ssi2*) as well as other pathogen signaling mutants (Fig. S11). The similarities between *p5cs1*-affected and light-affected gene expression were consistent with the relationship to chloroplast and photosynthesis gene expression described above. The similarities to pathogen and SA-related gene expression were consistent with recent data on the role of proline metabolism in pathogen resistance (Cecchini et al., 2011; Senthil-Kumar et al., 2012). However, it should be noted that these similarities in gene expression were somewhat limited and *p5cs1-4*

had an overall pattern of gene expression that was distinct from any of the datasets included in the Genevestigator analysis.

***p5cs1-4* mRNA sequencing identifies additional lipid metabolism genes which influence proline accumulation**

Given our findings of altered proline accumulation in *cyp86a2* and *lacs2-1* mutants, we searched the *p5cs1-4* RNA sequencing data for genes related to VLCFAs, cuticle or wax synthesis, or other genes related to fatty acid metabolism that have different read counts in *p5cs1-4* compared to wild type (Table S11). Interestingly *ACCD* (*ATCG00500*), which encodes a subunit of the acetyl-CoA carboxylase complex responsible for the first step of fatty acid synthesis in plastids (Li-Beisson et al., 2013), had 14-fold higher RPKM in stressed *p5cs1-4* compared to wild type (this difference was marginally non-significant in our statistical analysis). The Acetyl-CoA Carboxylase (ACC) complex consists of several nuclear encoded subunits in addition to the chloroplast encoded *ACCD*. We isolated a T-DNA mutant of the nuclear encoded ACC alpha subunit (*CAC3*, *At2g38040*) as a way to decrease activity of the ACC complex. The *cac3* mutant had a nearly 30% increase in proline accumulation at low ψ_w (Fig. 7F).

RPKM differences were also found for several genes encoding 3-ketoacyl-CoA synthases (*KCS*). In this case the fact that several *KCS* genes had putatively altered expression (Table S11) suggested that functional redundancy may mask phenotypes of single *kcs* mutants. Instead, we used the KCS inhibitor cafenstrole which has been shown to block KCS activity (Trenkamp et al., 2004; Nobusawa et al., 2013). Cafenstrol treatment increased proline content of unstressed seedlings nearly 3-fold and increased proline accumulation at low ψ_w by more than 40% (Fig. 7G). Both KCS and the ACC complex act upstream or in a different branch of VLCFA metabolism compared to *LACS2* and *CYP86A2*. Thus, these results added further evidence that blocking flux through lipid metabolism at any of a number of steps leads to increased proline accumulation at low ψ_w . The *cac3* and cafenstrole data also indicated that build-up of lipid metabolism intermediates upstream of *LACS2* was not responsible for high proline phenotype of *cyp86a2-1* and *lacs2-1*.

Discussion

We present two major lines of evidence which show how proline metabolism is integrated into cellular metabolism, particularly the relationship of proline to lipid metabolism and relationship to redox metabolism of mitochondria and chloroplast. First, *cyp86a2* and *lacs2-1*, as well as disruptions of lipid metabolism or transport at other points (ACC complex, KCS, CED1, CYP86A4, MYB16 and MYB106), all led to increased proline accumulation at low ψ_w (summarized in Fig. 8). The high proline and high *PDHI_{pro}:LUC2* phenotypes of *cyp86a2* and *lacs2-1* could be partially or completely abolished by treatment with ROS scavengers. Similarly, *cyp86a2-1* and *lacs2-1* were more sensitive to activation of proline accumulation by reductant (DTT) or inhibited NADPH oxidase activity (DPI). Together these data indicated that an effect of altered VLCFA synthesis on redox status, rather than signaling function of CYP86A2, LACS2 or VLCFAs themselves, was the cause of increased *PDHI_{pro}:LUC2* expression and proline accumulation. In a complementary line of experiments, we discovered that disrupted proline synthesis in *p5cs1-4* altered the expression of chloroplast and mitochondrial genes related to redox metabolism. Two main conclusions emerge from these data. The first is that proline metabolism is both influenced by and influences cellular redox status via previously unknown coordination with multiple metabolic pathways. A second conclusion is that proline and lipid metabolism share dual roles under stress to help buffer cellular redox status while producing proline and cuticle lipids useful for drought tolerance.

We selected the *PDHI* promoter for forward genetic screening because it could serve as a sensor for alterations in both stress signaling and metabolic state. Both *cyp86a2* (4442-4) and *lacs2* (4255-1) mutants had increased *PDHI_{pro}:LUC2* expression, but not increased proline, in the unstressed control. In the wild type background, *PDHI_{pro}:LUC2* expression of unstressed seedlings could be fully repressed to the stress level simply by addition of the NADPH oxidase inhibitor DPI. The high *PDHI_{pro}:LUC2* expression of *cyp86a2* and *lacs2* mutants could likewise be repressed by DPI. Together these data show that *PDHI_{pro}:LUC2* indeed acted as a sensitive indicator of altered redox and metabolic state even under conditions where proline level itself was not changed. At low ψ_w DPI, AsA and DMTU had lesser, but still significant, effects, presumably because other stress-related signals were also acting on *PDHI_{pro}:LUC2* expression and proline accumulation. The *PDHI_{pro}:LUC2* system can be further used as a new tool to understand unknown redox, metabolic and stress signaling mechanisms.

It was of interest to note that there was not a complete correspondence between expression of the *PDH1_{pro}:LUC2* reporter and endogenous *PDH1* at low ψ_w . The two agreed very well in unstressed plants. At low ψ_w , however, the endogenous *PDH1* was fully repressed despite the high proline accumulation in *cyp86a2* and *lacs2* while the *PDH1_{pro}:LUC2* reporter was only partially repressed. It is possible that the *PDH1_{pro}:LUC2* construct may not incorporate all elements (such as the 3' UTR or *PDH1* coding region) responsible for stress repression of *PDH1*. Alternatively, there may be position dependent-regulation of the *PDH1* promoter that does not occur at the *PDH1_{pro}:LUC2* locus. While fortuitous, this partial decoupling of *PDH1* and *PDH1_{pro}:LUC2* at low ψ_w allowed a larger range of mutants affecting proline accumulation to be isolated. The *PDH1_{pro}:LUC2* system, and modifications of it that include more or differing sections of *PDH1*, can be used as a system to explore stress repression of *PDH1* more fully.

The *cyp86a2* and *lacs2* mutants had altered proline accumulation despite no difference in P5CS1 or PDH1 protein level nor any change in expression of the core proline metabolism genes. How proline and VLCFA metabolism are coordinated is part of a larger question of how redox state can be communicated between different subcellular compartments such as the ER, chloroplast, and mitochondria. Such mechanisms are little known and proline metabolism is a promising system to address such questions. Although, we must first more definitively answer fundamental questions such as where proline is synthesized (cytoplasm or chloroplast). It is also interesting to note that mutants of *PDH1*, *CYPP86A2* and *LACS2* all have pathogen resistance phenotypes (Xiao et al., 2004; Bessire et al., 2007; Cecchini et al., 2011; Senthil-Kumar and Mysore, 2012). Also, there were similarities between genes differentially expressed in *p5cs1-4* and genes differentially expressed in defense signaling and SA-related mutants (Fig. S10 and S11). For *pdh1* mutants, their altered pathogen resistance is due to proline and PDH1-dependent mitochondrial ROS production. Possibly, altered proline levels and redox status are involved in the pathogen resistance phenotypes of *cyp86a2* and *lacs2* and are at least partially responsible for the gene expression changes in *p5cs1-4*.

RNA sequencing of *p5cs1-4* further supported the coordination of proline and lipid metabolism and showed a striking effect of *p5cs1-4* on expression of genes involved in redox metabolism of the mitochondria and chloroplast. These results are consistent with those of Lovell et al. (2015) who conducted QTL mapping using a recombinant inbred line (RIL)

population constructed using Arabidopsis accessions Tsu and Kas which have contrasting levels of proline accumulation during drought. They found a significant cytoplasmic effect on proline accumulation and the most likely variation underlying this effect was in mitochondrial *NADH Dehydrogenase subunit 9 (NAD9)*. In our data, *NAD9* had 10-fold higher RPKM in *p5cs1-4* compared to wild type at high ψ_w and 3-fold higher at low ψ_w (Table S10). In addition, more than 15 other *NADs* and related genes had similar pattern of higher RPKM in *p5cs1-4* (Table S10). It is possible that *NAD* expression is up-regulated to compensate for the reduced proline level (and presumably reduced proline catabolism) in *p5cs1-4*. These data underscore the importance of the proline cycle to feed reductant into the mitochondria, and are consistent with other evidence showing the importance of mitochondrial metabolism in drought resistance (Pastore et al., 2007; Giraud et al., 2008; Zsigmond et al., 2008; Atkin and Macherel, 2009; Rasmusson and Wallstrom, 2010; Skirycz et al., 2010; Schertl et al., 2014).

Under both high and low ψ_w there was a striking enrichment of chloroplast encoded genes among genes differentially expressed in *p5cs1-4*. This included genes involved in chloroplast protein translation as well as genes directly involved in the light reactions and NADPH metabolism. How and why disrupting proline metabolism had such a striking effect on chloroplast gene expression is not as immediately clear as the connection of proline to mitochondrial metabolism. However, the gene expression differences we saw in *p5cs1-4* are broadly consistent with the idea that proline metabolism may have a role in consuming NADPH and regenerating NADP^+ to provide a continued supply of electron acceptors for chloroplast electron transport (Sharma et al., 2011) and observations that proline accumulation and proline metabolism gene expression are modulated by light (Hayashi et al., 2000; Abraham et al., 2003). The fact that effects of *p5cs1-4* on chloroplast gene expression could be seen even in unstressed plants implies that flux through the cycle of proline synthesis and catabolism is high enough to impact chloroplast function even when proline levels are low. Further interpretation of this data is limited by the dearth of knowledge of metabolic flux through proline metabolism, unclear subcellular localization of P5CS1 and lack of data on whether proline metabolism mutants have reduced photosynthetic efficiency. In chloroplasts, enzyme activities are coordinated with redox status via modification of protein disulfide bond status by ferredoxins and thioredoxins (Meyer et al., 2012). It will be of interest to further investigate how redox metabolism in the chloroplast could be coordinated with proline synthesis which likely (although not for certain) occurs in the

cytoplasm. Likewise, it has been suggested the mammalian P5CS may be regulated by thioredoxins (Liang et al., 2013). Whether or not similar regulation exists in plants has, to our knowledge, not been investigated. Our *p5cs1-4* transcriptome data makes further experiments to uncover the specific mechanisms underlying the redox-proline and proline-photosynthesis connections even more compelling.

To our knowledge, there is little or no data directly comparable to our transcriptome analysis of *p5cs1-4*. Perhaps the most closely related work is that of Satoh et al. (2002) who reported genes induced by exogenous proline. We may expect that these genes would be less expressed in stressed *p5cs1-4* which has greatly decreased proline levels compared to wild type. Indeed, 5 out of the 20 proline-inducible genes with a ProRE reported by Satoh et al. (2002) were less expressed in *p5cs1-4* (Table S8); however, three such genes were upregulated in *p5cs1-4* (Table S9). Satoh et al. (2002) also found other genes responsive to proline but lacking a ProRE. However, the identity of these genes was not reported, precluding further comparison with our data. Whether *PDHI* and the ProRE are regulated directly by proline level via some unknown proline sensing mechanism or respond indirectly to other metabolic or redox-related signaling factors, as suggested by our analysis of *cyp86a2* and *lacs2* mutants, will be a question of interest as we characterize additional mutants from the *PDHI_{pro}:LUC2* screen.

We observed that the NADPH oxidase inhibitor DPI caused a massive increase in proline content of unstressed seedlings and suppressed *PDHI_{pro}:LUC2* expression in wild type as well as *cyp86a2* and *lacs2* mutants. These data indicate how redox status, possibly including redox status of the NADPH pool or ROS signaling, may be involved in adjusting proline metabolism to match cellular redox and metabolic state. However, our result differs from that of Ben Rejeb et al. (2015) who saw no effect of DPI on proline accumulation of unstressed plants. Their experiments were conducted on media containing sucrose which could have altered metabolite levels and redox status and thus obscured the DPI proline response.

The hypothesis that proline metabolism is regulated by redox or metabolic factors as well as abiotic stress has been proposed and discussed in several places (Szabados and Savoure, 2010; Verslues and Sharma, 2010; Sharma et al., 2011; Servet et al., 2012; Liang et al., 2013; Ben Rejeb et al., 2014; Giberti et al., 2014; Zhang and Becker, 2015) but experimental data to support such hypotheses has been limited. The *PDHI_{pro}:LUC2* mutant screen has revealed an

unexpected coordination of proline and lipid metabolism with altered cellular redox status being one of the factors allowing coordinate regulation of these pathways. Likewise, the gene expression data set reported here greatly strengthens hypotheses that the proline cycle is a significant determinant of chloroplast and mitochondria metabolism even when proline level is low. Our study demonstrates the need to mechanistically understand the redox-dependent regulation of proline metabolism. For example whether proline metabolism proteins undergo redox-sensitive post-translational modifications that affect their activity or whether the transcriptional regulation of *PDH1* transcription includes redox-sensitive factors. The *PDH1_{pro}:LUC2* screen and characterization of additional mutants promises to provide further new insights into proline metabolism, its regulation, and roles in stress resistance.

Materials and Methods

Construction of *PDH1_{pro}:LUC2*, mutagenesis and screening

A 1511 bp fragment encompassing the *PDH1* promoter out to -1389 bp and the 5' UTR (122 bp) of the *PDH1* transcript was amplified using primers to add Pst1 and Sal1 cloning sites (primer sequences are in Table S12). This promoter fragment was chosen because it was similar in length to the *PDH1* promoter fragment we previously used to analyze *PDH1*promoter:GUS expression (Sharma et al., 2011) and contains the ProRE described by Satoh et al., (2002) as well as several other potential cis- elements (Nakashima et al., 1998). This fragment was 112 bp shorter than the *PDH1* promoter fragment we previously used for *promoter:GUS* analysis (Sharma et al., 2011) to avoid a Sal1 site which interfered with cloning. The amplified fragment was ligated into pJET1.2 blunt cloning vector (ThermoFisher Scientific) and confirmed by sequencing. The *PDH1* promoter fragment was then cloned into pCAB2-LUC2-pCAMBIA1390 (Wang et al., 2011a) containing the pGL4.10-LUC2 (Promega) Luciferase2 sequence. pCAB2-LUC2-pCAMBIA1390 was Sal1/Pst1 digested and gel purified to remove the CAB2 promoter and then ligated with the Pst1-*PDH1* promoter-Sal1 fragment. The resulting plasmid was transformed into *Agrobacterium tumefaciens* strain GV3101 by electroporation and used to transform Col-0 wild type by floral dip method. T₂ lines having 3:1 segregation ratio consistent with a single locus insertion were selected and homozygous T₃ plants confirmed by antibiotic screening. These lines were further tested for similar repression of *PDH1_{pro}:LUC2* during low Ψ_w and induction of *PDH1_{pro}:LUC2* expression upon stress release as the endogenous *PDH1*. A

single transgenic line was selected for mutagenesis. Subsequent genome sequencing confirmed that this line has insertion of the *PDHI_{pro}:LUC2* construct adjacent to position 11887500 of chromosome 1.

Approximately 60,000 T₃ seeds of this line were EMS mutagenized following standard protocols (Weigel and Glazebrook, 2006). Mutagenized seed were sown in large pots (approximately 60-70 seed per pot). M₁ seed from each pot was collected together as a pool resulting in more than 900 pools of mutagenized seed. From each of these pools, 100 seed were sterilized and plated in a grid pattern on 140 mm diameter plates in which the agar had been overlaid with nylon mesh to facilitate seedling transfer. The media used was our laboratory standard media of half strength Murashige-Skoog (MS) salts with 2 mM MES (pH 5.7) buffer but no sugar (Sharma et al., 2011). Each plate also included 3-5 unmutagenized *PDHI_{pro}:LUC2* seed for comparison. After stratification for 4 days, plates were incubated vertically in a growth chamber (23° C, light intensity of 100 $\mu\text{mol m}^{-1} \text{sec}^{-1}$) for seven days. On the seventh day, plates were sprayed with 1 mM luciferin and imaged using a Xenogen Ivis system (Perkin Elmer). Seedlings having high or low luciferase activity were marked. Seedlings were then transferred to low ψ_w PEG-infused agar plates (-1.0 MPa) for 4 days and luciferase activity imaged again. PEG-agar plates were prepared as previously described (Verslues et al., 2006; Sharma et al., 2011) with the relative volumes of agar and PEG overlay adjusted for the larger size plates.

Seedlings having high or low luciferase activity either before or after the stress treatment were transferred to soil. Seed from these plants (M₂ generation) was then used for a secondary screen conducted in the same manner but with 5-8 seedlings per line imaged and luciferase activity quantified (using the Xenogen Ivis software). Several hundred putative mutants were rescreened in the M₂ generation and more than 30 lines with consistently high *ProDH1_{pro}:LUC2* activity and a smaller set of mutants with low *ProDH1_{pro}:LUC2* (approximately 7, although some are still being verified) selected for further analysis. Mutants having the greatest difference in luciferase activity compared to the wild type were selected for further analysis including backcrosses, complementation testing, crosses to Landsberg *erecta* for mapping and, further phenotypic analysis.

Whole Genome sequencing, SNP calling and Next Generation Mapping

Mutants having high *PDH1_{pro}:LUC2* were crossed to *Ler* and resulting F₂ seed plated as described above. Mutants in which the high *PDH1_{pro}:LUC2* phenotype segregated in a 3:1 ratio consistent with a single recessive locus were considered suitable for sequencing analysis (in most cases the recessive nature of the mutation was also confirmed during backcrossing to unmutagenized *PDH1_{pro}:LUC2*). Genomic DNA was extracted from a pool of 80-100 homozygous mutant seedlings selected from the F₂ population based on their high *PDH1_{pro}:LUC2* expression. DNA was extracted using Qiagen Plant DNAeasy kit and purity of the DNA extracts tested by absorbance measurements and agarose gel analysis.

For whole genome sequencing, six mutant DNA pools were prepared using Illumina TruSeq DNA library construction. Briefly, 1 µg of each DNA pool was sheared to fragments of 150~500 bp using a Covaris M220 Focused-ultrasonicator with the 200 bp program. The sheared DNA was size enriched by double-sided Solid Phase Reversible Immobilization (SPRI) using an Agencourt AmPure XP kit. A TruSeq DNA LT Sample Prep Kit (Illumina) was used to perform end repair, A-tailing, and adaptor ligation. The barcoded samples were then amplified by 8 cycles of PCR and cleaned up by Ampure XP beads (Beckman Agencourt). The absolute concentrations and profiles of the libraries were determined by Qubit (Invitrogen) and BioAnalyzer High Sensitivity DNA chip (Agilent), respectively. The final library sizes range from 250-750bps with major size of 350bp. The molar concentrations of the libraries were derived by qPCR normalization using the KAPA NGS Library qPCR kit. Multiplexed sequencing was conducted on one lane of PE2*101 on an Illumina HiSeq2500. The Illumina CASAVA 1.8.2 pipeline was applied for barcode demultiplexing and generating fastq files. The Illumina sequencing and initial data processing were conducted by the High Throughput Genomics Core facility of the Biodiversity Research Center, Academia Sinica.

After sequencing, reads were mapped to the TAIR10 genome (ftp://ftp.arabidopsis.org/home/tair/Genes/TAIR10_genome_release/) using Bowtie2 (Langmead and Salzberg, 2012) and BLAT (Kent, 2002), and SNP calling was conducted by the RackJ software package (<http://rackj.sourceforge.net/>). Mapping results in BAM format were processed into pileup files using Samtools v0.1.16 and then emap files as instructed in the Next Generation Mapping website (<http://bar.utoronto.ca/NGM/>). The processed emap files were

analyzed using the Next Generation Mapping analysis tool (<http://bar.utoronto.ca/NGM/>) described in Austin et al., (2011).

Phenotypic analyses and T-DNA mutants

Seeds of T-DNA mutants were obtained from the Arabidopsis Biological Resource Center and homozygous plants were confirmed by PCR genotyping using primers from the Signal (www.signal.salk.edu) data base. RT-PCR was used to confirm absence of transcript in each new mutant (Fig S12; genotyping and RT-PCR primers are given in Table S12) Seeds for *lacs2-1* and *lacs3-1* were provided by the laboratory of Dr. John Browse (Washington State University). The proline metabolism mutants *p5cs1-4* and *pdh1-2* have been previously verified by our laboratory (Sharma and Verslues, 2010; Sharma et al., 2011). For transgenic complementation of 4442-4, full length cDNA sequence of *CYP86A2* was amplified from total RNA (primers given in Table S12), and cloned into pDONOR 207 by BP reaction. For plant expression, the clone was moved into pEG100 (Earley et al., 2006) and transformed into *Agrobacterium tumefaciens* GV3101, and the 4442-4 EMS mutant transformed by the floral dip method.

Free proline was quantified using Ninhydrin assay (Bates et al. 1973) adapted to 96 well plate format (Verslues, 2010). For pharmacological treatments, seedlings were pretreated with ascorbic acid (Sigma), N,N'-Dimethylthiourea (ACROS Organics) or Diphenylene iodonium (Sigma) for 24 h and then transferred to low ψ_w (-1.2 MPa, 96h) with the same concentration of the chemical. Cafenstrole (Wako Chemical) treatment was performed in the same manner but without pretreatment before transfer to low ψ_w . Western blotting of P5CS1 and PDH1 was performed using antisera generated by our laboratory as previously described (Kesari et al., 2012; Bhaskara et al., 2015). For Toluidine Blue staining, whole seedlings or leaves were submerged in an aqueous solution of 0.05% (w/v) toluidine blue for 2-5 minutes. Excess stain removed by rinsing with sterile distilled water before being photographed using a Lumar v12 stereoscope (Zeiss). For RT-PCR and quantitative RT-PCR analysis, total RNA was extracted from seedlings using RNeasy plant mini kit (Qiagen). Quantitative PCR was performed using KAPA SYBR FAST Master Mix (KAPABiosystems) on a QuantStudio 12K Flex Real-Time PCR System (Applied Biosystems). NADPH and NADPH were measured using an analysis kit (BioAssay Systems, Hayward, CA) with sample collection and extraction performed as

previously described (Sharma et al., 2011). ROS staining used 2', 7'-dichlorodihydrofluorescein diacetate (H2DCFDA) dye with excitation at 488 nm and emission at 500–550 nm with images analyzed on a Zeiss LSM510 Meta microscopy system.

mRNA sequencing

mRNA sequencing was carried out by the High Throughput Genomics Core facility of the Biodiversity Research Center, Academia Sinica following protocols provided by Illumina including mRNA-seq library preparation, addition of MID barcodes to the ds cDNA fragments and volume adjustment. Using the Illumina mRNA-seq kit, 10-15 ug of total RNA was for isolation of poly-A RNA by oligo-dT beads and subjected to cation-catalyzed fragmentation for four minutes at 94°C. The mRNA fragments were then converted into ds cDNA by random priming, and the ends were repaired and A-tailed. Multiplexing barcodes were then added to the DNA fragment ends with modifications from the paired-end gDNA library prep kit. The ligation products were size-selected on agarose gel (200-400 bp), subjected to 18 cycles of PCR and cleaned up by Ampure beads (Beckman Agencourt). The absolute concentrations of the libraries were determined fluorometrically by Qubit (Invitrogen) and BioAnalyzer High Sensitivity DNA chip (Agilent).

Mixing of the differentially barcoded samples for each lane was based on qPCR-derived relative concentration for amplifiable fraction of each library. Briefly, the relative amplifiable concentration of each library was estimated by real-time PCR analyses (Roche Light Cycler 480) using the KAPA NGS Library qPCR kit (KAPA) by regression to the curve generated using the included standard of known concentration. Correlations between output clusters and qPCR concentrations were derived by plotting the relative concentrations of previously sequenced PhiX control and libraries against the output cluster numbers. The relative concentrations of the MID libraries were then estimated by regression. The amount (fmoles) of each library to be mixed in a pool for each lane was determined based on the proportion each would account for in the projected output clusters (i.e. estimating the fmoles required per library for generating $300,000/8 = 37,500$ raw clusters per tile if the lane to be used for sequencing a pool of 8 barcodes). The sequencing was performed on an Illumina Genome Analyzer IIx in the High Throughput Sequencing Core Facility of Academia Sinica, and 73-nt reads obtained. Base calling and demultiplexing were performed using CASAVA and bclfastq1.6.

RPKM values were calculated using the RackJ software package (<http://rackj.sourceforge.net/>) with reads mapped to the TAIR10 genome using BLAT (Kent, 2002). RPKM values of control and treatment samples were compared using Z-statistic as described in Lan et al. (2013). GO enrichment was computed using TopGO elim method (Alexa et al., 2006) using GOBU with its MultiView plugin (Lin et al., 2006).

Accession numbers

mRNA sequencing results are available under Gene Expression Omnibus accession number GSE75933.

Supplemental Material

Figure S1: Example of primary screen plate images using EMS mutagenized *PDH1_{pro}:LUC2*.

Figure S2: NGM analysis and identification of *CYP86A2* and *LACS2* as the causative mutated genes in the 4442-2 and 4255-1 EMS mutants

Figure S3: *PDH1_{pro}:LUC2* crossed to *cyp86a2-1* and *lacs2-1* T-DNA mutants shows the same high *PDH1_{pro}:LUC2* phenotype as the 4244-2 and 4255-2 EMS mutants

Figure S4: Expression of proline synthesis and catabolism genes in *cyp86a2* mutants.

Figure S5: NADP⁺ and NADPH analysis of wild type, *cyp86a2-1* and *lacs2-1*.

Figure S6: ROS levels of wild type, *cyp86a2-1* and *lacs2-1*.

Figure S7: MapMan analysis of photosynthesis-related gene expression in stress and control treated wild type as well as *p5cs1-4* compared to wild type in unstressed and low water potential (-1.2 MPa, 96 h) treatments.

Figure S8: MapMan analysis of mitochondrial electron transport-related gene expression in stress and control treated wild type as well as *p5cs1-4* compared to wild type in unstressed and low water potential (-1.2 MPa, 96 h) treatments.

Figure S9: MapMan analysis of amino acid metabolism-related gene expression in *p5cs1-4* compared to wild type in unstressed and low water potential (-1.2 MPa, 96 h) treatments.

687 Fig S10: Differentially expressed genes in *p5cs1-4* control vs. W.T. control compared to public
688 microarray data using the Genevestigator Signature analysis tool.

689 Fig S11: Differentially expressed genes in *p5cs1-4* stress vs. W.T. stress compared to public
690 microarray data using the Genevestigator Signature analysis tool.

691 Figure S12: RT-PCR check of lipid- and cuticle-related T-DNA mutants.

692 Table S1: RPKM values from RNA sequencing analysis of wild type (Col-0) and *p5cs1-4* under
693 either control (-0.25 MPa) or stress (transfer to -1.2 MPa for 96 h)

694 Table S2: Genes with increased expression in Col-0 wild type at 96 h after transfer to low water
695 potential (-1.2 MPa) stress and GO terms significantly enriched in the up-regulated genes.

696 Table S3: Genes with decreased expression in wild type at 96 h after transfer to low water
697 potential (-1.2 MPa) stress and significantly enriched GO terms among the down-regulated
698 genes.

699 Table S4: Genes with increased expression in unstressed *p5cs1-4* compared to unstressed wild
700 type along with significantly enriched GO terms.

701 Table S5: Genes with decreased expression in unstressed *p5cs1-4* compared to unstressed wild
702 type along with significantly enriched GO terms.

703 Table S6: Genes with increased expression in stressed (-1.2 MPa, 96 h) *p5cs1-4* compared to
704 stressed wild type along with significantly enriched GO terms.

705 Table S7: Genes with decreased expression in stressed (-1.2 MPa, 96 h) *p5cs1-4* compared to
706 stressed wild type along with significantly enriched GO terms.

707 Table S8: Both stress-responsive and non-responsive genes are among those up-regulated in
708 *p5cs1-4*.

709 Table S9: Both stress-responsive and non-responsive genes are among those down-regulated in
710 *p5cs1-4*.

Table S10: Chloroplast and mitochondrial NAD(P)H dehydrogenase genes with putatively altered expression in *p5cs1-4*.

Table S11: Lipid and wax metabolism genes with putatively altered expression in *p5cs1-4*.

Table S12: Primer sequences used in this study.

Acknowledgements

We thank the laboratory of Shu-Hsing Wu for the pCAB2-LUC2-pCAMBIA1390 plasmid, John Browse (Washington State University) for the *lacs2* and *lacs3* mutants, Mei-Yeh Liu and the High Throughput Genomics Core, Biodiversity Research Center, Academia Sinica for sequencing services, Mei-Jane Fang for assistance with luciferase imaging and microscopy, Ang-Hsi Lin for mutant screening and Srilakshmi Mukiri and Trent Z. Chang for laboratory assistance.

Figure Legends

Figure 1: A *PDHI_{pro}:LUC2* reporter responsive to low ψ_w .

A. The *PDHI* promoter and 5' UTR were fused to the *Luciferase2* (*LUC2*) coding region and used to generate transgenic plants. Quantitation of *PDHI_{pro}:LUC2* luminescence in shoot tissue of seedlings transferred to low ψ_w (-1.0 MPa) for the indicated lengths of time is shown. Data are means \pm S.E. (n=6).

B. Representative false color images of luminescence intensity from experiments reported in

A. Intensity scale for the images is shown at right.

Figure 2: Mutants 4442-4 and 4255-1 have increased *PDHI_{pro}:LUC2* activity and increased proline accumulation at low ψ_w .

A. Representative false color luminescence images of wild type and mutants in the unstressed control and after 96 h at -1.0 MPa low ψ_w treatment.

B. Quantification of *PDHI_{pro}:LUC2* activity in 4442-1 and 4255-1. Data are means \pm S.E. (n=4-15). Significant differences ($p \geq 0.05$) compared to wild type in the same treatment are marked (*). Luminescence intensities are given in photons (p) per second (s) per cm^2 per steradian (sr).

C. Proline accumulation unstressed control (-0.25 MPa) or low ψ_w stress (-1.2 MPa) for wild type (W.T.) and mutants. Data are means \pm S.E. (n=3-9). Significant differences ($p \geq$

0.05) compared to wild type in the same treatment are marked (*). Note for W.T. is the unmutagenized *PDH1_{pro}:LUC2* line for all experiments in panels A-C.

- D. *PDH1* gene expression in Col-0 wild type, 4442-4 and two T-DNA alleles of *cyp86a2* in the unstressed control treatment or at 96 h after transfer to -1.2 MPa stress. Data are means \pm S.E. (n=3). Significant differences ($p \geq 0.05$) compared to wild type in the same treatment are marked (*). Expression of additional proline metabolism genes in these mutants is shown in Supplemental Figure S4.

Figure 3: 4442-4 and 4255-1 are alleles of *cyp86a2* and *lacs2*, respectively.

- A. Proline accumulation in two *cyp86a2* T-DNA alleles and *lacs2-1* under control and -1.2 MPa low ψ_w stress. Data are means \pm S.E. (n=4-6) from two experiments. Significant differences ($p \geq 0.05$) compared to wild type in the same treatment are marked (*).
- B. *PDH1_{pro}:LUC2* imaging in F₁ seedlings of crosses of 4442-1 and 4255-1 with *cyp86a2-1* and *lacs2-1*, respectively, along with W.T. *PDH1_{pro}:LUC2* and mutant seedlings as controls.
- C. Toluidine blue staining using seedlings of Col-0, W.T. *PDH1_{pro}:LUC2* as well as mutants and a transgenic complemented line of 4442-4.
- D. *PDH1_{pro}:LUC2* imaging of W.T. *PDH1_{pro}:LUC2*, 4442-4 and 4442-4 complemented with *35S:CYP86A2*. Stress treatment was -1.0 MPa for 96 h.
- E. Stress-induced (-1.2 MPa, 96 h) proline accumulation in 4442-4 and two independent T₃ lines of 4442-4 complemented with *35S:CYP86A2*. Data are means \pm S.E. (n=4-6) from two experiments. Significant differences ($p \geq 0.05$) compared to wild type in the same treatment are marked (*).
- F. RT-PCR analysis of Col-0, W.T. *PDH1_{pro}:LUC2*, *lacs2-1* and 4255-1 using primers to amplify the full length LACS2 RNA or the region around Intron 10. *ACT8* was used as a reference gene.

Figure 4: Effects of *cyp86a2* and *lacs2* mutants on proline metabolism and identification of additional cuticle lipid-related mutants with increased proline accumulation at low ψ_w .

- A. Western blot of PDH1 and P5CS1 protein levels in Col-0, W.T. *PDH1_{pro}:LUC2* and *cyp86a2* and *lacs2* mutants. *p5cs1-4* and *pdh1-2* were included to show the specificity of the antisera. Blots were stripped and reprobed with antisera recognizing HSC70 as a loading control. 50 μ g of protein was loaded in each lane.

- B. Effect of a range of low ψ_w , salt, or ABA treatments on proline accumulation of Col-0 wild type and *cyp86a2* mutants. Data are means \pm S.E. (n=8-12) from two experiments. Significant differences ($p \geq 0.05$) compared to wild type in the same treatment are marked (*).
- C. Stress-induced (-1.2 MPa, 96 h) proline accumulation in cuticle metabolism mutants. Data are means \pm S.E. (n=11-24) from two experiments. Significant differences ($p \geq 0.05$) compared to wild type are marked (*). For *ced1*, *cyp77a6* and *cyp86a4* the data shown are combined from 2-3 T-DNA alleles which showed identical phenotype. Additional information and RT-PCR verification of T-DNA mutants can be found in Fig S10.

Figure 5: Effect of DTT and reactive oxygen scavengers AsA and DMTU on proline accumulation and *PDHI_{pro}:LUC2* activity.

- A. Effect of DTT treatment on proline accumulation of seedlings at high ψ_w . Data are means \pm S.E. (n=10-44) combined from three experiments. Significant differences ($p \geq 0.05$) compared to wild type in the same treatment or between 0 and 5 mM DTT treatment of wild type are marked (*).
- B. Effect of DTT treatment at -1.2 MPa on proline accumulation. Data are means \pm S.E. (n=10-44) combined from three experiments. Significant differences ($p \geq 0.05$) compared to wild type are marked (*).
- C. Effect of AsA and DMTU on proline levels at -0.25 and -1.2 MPa. Data are means \pm S.E. (n=10-44) combined from three experiments. Significant differences ($p \geq 0.05$) compared to the mock treatment are marked (*).
- D. Effect of AsA on *PDHI_{pro}:LUC2* activity in wild type, 4442-4 and 4255-1 at high (-0.25 MPa) or low ψ_w (-1.2 MPa). Data are means \pm S.E. (n=10-44) combined from three experiments. Significant differences ($p \geq 0.05$) compared to the mock treatment are marked (*).
- E. Effect of DMTU on *PDHI_{pro}:LUC2* activity in wild type, 4442-4 and 4255-1. Data are means \pm S.E. (n=10-44) combined from three experiments. Significant differences ($p \geq 0.05$) compared to the mock treatment are marked (*).
- F. False color imaging of *PDHI_{pro}:LUC2* activity in representative seedlings from the experiments reported in E.

Figure 6: Effect of DPI on proline accumulation and *PDHI_{pro}:LUC2* activity.

- A. Effect of DPI (2.5 μ M) on proline accumulation of seedlings at high (-0.25 MPa) or low (-1.2 MPa) ψ_w . Data are means \pm S.E. (n=14-18) combined from three experiments. Significant differences ($p \geq 0.05$) compared to wild type (Col-0) in the same treatment or between mock and DPI treatment of Col-0 are marked (*).
- B. Effect of DPI on *PDHI_{pro}:LUC2* activity in wild type, 4442-4 and 4255-1 at high (-0.25 MPa) or low (-1.2 MPa) ψ_w . Data are means \pm S.E. (n=10-44) combined from three experiments. Significant differences ($p \geq 0.05$) compared to the mock treatment are marked (*).
- C. False color imaging of *PDHI_{pro}:LUC2* activity in representative seedlings from the experiments reported in B.

Figure 7: RNA sequencing of Col-0 wild type and *p5cs1-4* shows the effect of proline on chloroplast and mitochondria metabolism and identifies additional lipid metabolism loci affecting proline accumulation.

- A. Plot of RPKM values for Col-0 in the unstressed control versus Col-0 after 96 h low ψ_w (-1.2 MPa) treatment. Significantly up- or down-regulated genes are indicated by red or blue circles, respectively while other data points are plotted in grey. Complete listing of RPKM values can be found in Supplemental Table S1 and lists of significantly up or down regulated genes as well as significantly enriched GO terms can be found in Supplemental Tables S2 and S3.
- B. Plots of RPKM values for *p5cs1-4* versus Col-0 wild type in the unstressed control treatment and after 96 h low ψ_w treatment. Data presentation is as described for A. Complete listing of RPKM values can be found in Supplemental Table S1 and lists of significantly up or down regulated genes in *p5cs1-4* in both control and stress treatments along with listing of significantly enriched GO terms can be found in Supplemental Tables S4-S7.
- C. Comparison of low ψ_w up- or down-regulated genes identified by RNA sequencing to those identified by previous microarray analysis of the same stress treatment.
- D. Comparison of genes up- or down regulated in *p5cs1-4* in the control and low ψ_w stress treatment.

E. Comparison of fold change in gene expression detected by RNA sequencing versus fold change detected by QPCR for selected genes down-regulated in *p5cs1-4*. QPCR data are means \pm S.E. (n=5-6) from two experiments. Ratios significant different ($p \geq 0.05$) from 1 based on one sided T-test are indicated.

F. Proline levels in unstressed control (-0.25 MPa) or after 96 h low ψ_w treatment (-1.2 MPa) for Col-0 wild type and *cac3* mutant. Data are means \pm S.E. (n=15-18) from three experiments. Significant difference ($p \geq 0.05$) compared to wild type in the same treatment is marked (*). Effect of the KCS inhibitor cafenstrole on proline accumulation at high or low ψ_w . Data are means \pm S.E. (n=15-18) from three experiments. Significant differences ($p \geq 0.05$) compared to wild type in the same treatment are marked (*).

Figure 8: Summary diagram showing the core pathway of proline metabolism in relation to lipid, cuticle and redox-related genes found to affect proline accumulation.

Multiple genes and pharmacological treatments disrupting lipid metabolism or NADPH oxidase activity were found to affect proline accumulation and *PDH1_{pro}:LUC2* expression. This included *CYP86A2* and *LACS2* identified in the *PDH1_{pro}:LUC2* forward genetic screen; *CYP86A4*, *CED1*, *MYB16* and *MYB106* identified by reverse genetics; *CAC3* (chloroplast Acetyl CoA Carboxylase complex) and *KCS* genes identified by *p5cs1-4* RNA sequencing as well as strong effects of the NADPH Oxidase inhibitor DPI. The reactions catalyzed by these proteins are spread across several compartments including endoplasmic reticulum (ER), chloroplast and plasma membrane (PM). The commonality among these pathways and proline metabolism itself is an effect on redox status by the consumption of NADPH and regeneration of NADP⁺, either directly as for P5CS1, P5CR, LACS2, CYP86A2 and NADPH oxidases, or indirectly by modifying the flux through lipid synthesis as for CAC3, KCS, CED1, MYB16 and MYB106. This commonality, along with data obtained with ROS scavengers and DTT treatment, indicates that redox status is a key factor linking these pathways together. Consistent with this, RNA sequencing data showed that *p5cs1-4* had substantial alterations in gene expression related chloroplast and mitochondrial redox metabolism further indicating the relationship of proline to redox status. The similar effects of *p5cs1-4* on gene expression at both high and low ψ_w indicated the importance of proline metabolism, and likely a high rate of flux through the proline cycle of synthesis and catabolism, even in unstressed plants where proline level is low. P5CS1 is

drawn in its own box to indicate that its subcellular localization is unclear. How changes in redox state are communicated between these subcellular compartments is unknown.

References

- Abraham E, Rigo G, Szekely G, Nagy R, Koncz C, Szabados L (2003) Light-dependent induction of proline biosynthesis by abscisic acid and salt stress is inhibited by brassinosteroid in *Arabidopsis*. *Plant Molec Biol* 51: 363-372
- Alexa A, Rahnenfuhrer J, Lengauer T (2006) Improved scoring of functional groups from gene expression data by decorrelating GO graph structure. *Bioinformatics* 22: 1600-1607
- Atkin OK, Macherel D (2009) The crucial role of plant mitochondria in orchestrating drought tolerance. *Ann Bot* 103: 581-597
- Austin RS, Vidaurre D, Stamatiou G, Breit R, Provart NJ, Bonetta D, Zhang JF, Fung P, Gong YC, Wang PW, McCourt P, Guttman DS (2011) Next-generation mapping of *Arabidopsis* genes. *Plant J* 67: 715-725
- Ben Rejeb K, Abdelly C, Savoure A (2014) How reactive oxygen species and proline face stress together. *Plant Physiol Biochem* 80: 278-284
- Ben Rejeb K, Benzarti M, Debez A, Bailly C, Savoure A, Abdelly C (2015) NADPH oxidase-dependent H₂O₂ production is required for salt-induced antioxidant defense in *Arabidopsis thaliana*. *J Plant Physiol* 174: 5-15
- Ben Rejeb K, Lefebvre-De Vos D, Le Disquet I, Leprince AS, Bordenave M, Maldiney R, Jdey A, Abdelly C, Savoure A (2015) Hydrogen peroxide produced by NADPH oxidases increases proline accumulation during salt or mannitol stress in *Arabidopsis thaliana*. *New Phytol* 208: 1138-1148
- Bessire M, Chassot C, Jacquat AC, Humphry M, Borel S, Pet  tot JMC, M  traux JP, Nawrath C (2007) A permeable cuticle in *Arabidopsis* leads to a strong resistance to *Botrytis cinerea*. *EMBO J* 26: 2158-2168
- Bhaskara GB, Yang TH, Verslues PE (2015) Dynamic proline metabolism: importance and regulation in water limited environments. *Frontiers in Plant Sci* 6
doi.org/10.3389/fpls.2015.00484
- Bussis D, Heineke D (1998) Acclimation of potato plants to polyethylene glycol-induced water deficit - II. Contents and subcellular distribution of organic solutes. *J Exp Bot* 49: 1361-1370
- Cecchini NM, Monteoliva MI, Alvarez ME (2011) Proline dehydrogenase contributes to pathogen defense in *Arabidopsis*. *Plant Physiol* 155: 1947-1959
- de Ronde JA, Cress WA, Kruger GHJ, Strasser RJ, Van Staden J (2004) Photosynthetic response of transgenic soybean plants, containing an *Arabidopsis* P5CR gene, during heat and drought stress. *J Plant Physiol* 161: 1211-1224
- Dietrich K, Weltmeier F, Ehlert A, Weiste C, Stahl M, Harter K, Droge-Laser W (2011) Heterodimers of the *Arabidopsis* Transcription Factors bZIP1 and bZIP53 Reprogram Amino Acid Metabolism during Low Energy Stress. *Plant Cell* 23: 381-395
- Earley KW, Haag JR, Pontes O, Opper K, Juehne T, Song KM, Pikaard CS (2006) Gateway-compatible vectors for plant functional genomics and proteomics. *Plant J* 45: 616-629
- Funck D, Eckard S, Muller G (2010) Non-redundant functions of two proline dehydrogenase isoforms in *Arabidopsis*. *BMC Plant Biol* 10: 70

907 Funck D, Winter G, Baumgarten L, Forlani G (2012) Requirement of proline synthesis during
 908 Arabidopsis reproductive development. *BMC Plant Biol* 12: 1-12
 909 Giberti S, Funck D, Forlani G (2014) Delta(1)-pyrroline-5-carboxylate reductase from
 910 Arabidopsis thaliana: stimulation or inhibition by chloride ions and feedback regulation
 911 by proline depend on whether NADPH or NADH acts as cosubstrate. *New Phytol* 202:
 912 911-919
 913 Giraud E, Ho LHM, Clifton R, Carroll A, Estavillo G, Tan Y-F, Howell KA, Ivanova A, Pogson
 914 BJ, Millar AH, Whelan J (2008) The Absence of ALTERNATIVE OXIDASE1a in
 915 Arabidopsis Results in Acute Sensitivity to Combined Light and Drought Stress. *Plant*
 916 *Physiol.* 147: 595-610
 917 Gleeson D, Lelu-Walter MA, Parkinson M (2005) Overproduction of proline in transgenic
 918 hybrid larch (*Larix x leptoeuropaea* (Dengler)) cultures renders them tolerant to cold, salt
 919 and frost. *Molec Breed* 15: 21-29
 920 Hayashi F, Ichino T, Osanai R, Wada K (2000) Oscillation and regulation of proline content by
 921 P5CS and ProDH gene expressions in the light/dark cycles in Arabidopsis thaliana L.
 922 *Plant Cell Physiol* 41: 1096-1101
 923 Kavi Kishor PB, Hima Kumari P, Sunita MSL, Sreenivasulu N (2015) Role of proline in cell
 924 wall synthesis and plant development and its implications in plant ontogeny. *Frontiers in*
 925 *Plant Science* 6: doi.org/10.3389/fpls.2015.00544
 926 Kent WJ (2002) BLAT - The BLAST-like alignment tool. *Genome Research* 12: 656-664
 927 Kesari R, Lasky JR, Villamor JG, Marais DLD, Chen YJC, Liu TW, Lin W, Juenger TE,
 928 Verslues PE (2012) Intron-mediated alternative splicing of Arabidopsis P5CS1 and its
 929 association with natural variation in proline and climate adaptation. *Proc Natl Acad Sci*
 930 *USA* 109: 9197-9202
 931 Kolbe A, Oliver SN, Fernie AR, Stitt M, van Dongen JT, Geigenberger P (2006) Combined
 932 transcript and metabolite profiling of Arabidopsis leaves reveals fundamental effects of
 933 the thiol-disulfide status on plant metabolism. *Plant Physiol* 141: 412-422
 934 Lan P, Li WF, Lin WD, Santi S, Schmidt W (2013) Mapping gene activity of Arabidopsis root
 935 hairs. *Genome Biol* 14: R67 DOI: 10.1186/gb-2013-14-6-r67
 936 Langmead B, Salzberg SL (2012) Fast gapped-read alignment with Bowtie 2. *Nat Meth* 9: 357-
 937 U354
 938 Less H, Galili G (2008) Principal Transcriptional Programs Regulating Plant Amino Acid
 939 Metabolism in Response to Abiotic Stresses. *Plant Physiol.* 147: 316-330
 940 Li-Beisson Y, Pollard M, Sauveplane V, Pinot F, Ohlrogge J, Beisson F (2009) Nanoridges that
 941 characterize the surface morphology of flowers require the synthesis of cutin polyester.
 942 *Proc Natl Acad Sci USA* 106: 22008-22013
 943 Li-Beisson Y, Shorrosh B, Beisson F, Andersson MX, Arondel V, Bates PD, Baud S, Bird D,
 944 DeBono A, Durrett TP, Franke RB, Graham IA, Katayama K, Kelly AA, Larson T,
 945 Markham JE, Miquel M, Molina I, Nishida I, Rowland O, Samuels L, Schmid KM, Wada
 946 H, Welti R, Xu C, Zallot R, Ohlrogge J (2013) Acyl-Lipid Metabolism. *The Arabidopsis*
 947 *Book*: e0161
 948 Liang XW, Zhang L, Natarajan SK, Becker DF (2013) Proline mechanisms of stress survival.
 949 *Antioxidants & Redox Signaling* 19: 998-1011
 950 Lin WD, Chen YC, Ho JM, Hsiao CD (2006) GOBU: Toward an integration interface for
 951 biological objects. *Journal of Information Science and Engineering* 22: 19-29

952 Mattioli R, Biancucci M, Lonoce C, Costantino P, Trovato M (2012) Proline is required for male
 953 gametophyte development in Arabidopsis. BMC Plant Biol 12: 1-16
 954 Meyer Y, Belin C, Delorme-Hinoux V, Reichheld JP, Riondet C (2012) Thioredoxin and
 955 glutaredoxin systems in plants: molecular mechanisms, crosstalks, and functional
 956 significance. Antioxidants & Redox Signaling 17: 1124-1160
 957 Miller G, Stein H, Honig A, Kapulnik Y, Zilberstein A (2005) Responsive modes of *Medicago*
 958 *sativa* proline dehydrogenase genes during salt stress and recovery dictate free proline
 959 accumulation. Planta 222: 70-79
 960 Nakashima K, Satoh R, Kiyosue T, Yamaguchi-Shinozaki K, Shinozaki K (1998) A gene
 961 encoding proline dehydrogenase is not only induced by proline and hypoosmolarity, but
 962 is also developmentally regulated in the reproductive organs of Arabidopsis. Plant
 963 Physiol 118: 1233-1241
 964 Nanjo T, Kobayashi M, Yoshiba Y, Kakubari Y, Yamaguchi-Shinozaki K, Shinozaki K (1999)
 965 Antisense suppression of proline degradation improves tolerance to freezing and salinity
 966 in Arabidopsis thaliana. Febs Lett 461: 205-210
 967 Nobusawa T, Okushima Y, Nagata N, Kojima M, Sakakibara H, Umeda M (2013) Synthesis of
 968 Very-Long-Chain Fatty Acids in the Epidermis Controls Plant Organ Growth by
 969 Restricting Cell Proliferation. PLoS Biol 11: e1001531
 970 Oshima Y, Shikata M, Koyama T, Ohtsubo N, Mitsuda N, Ohme-Takagi M (2013) MIXTA-Like
 971 transcription factors and WAX INDUCER1/SHINE1 coordinately regulate cuticle
 972 development in Arabidopsis and *Torenia fournieri*. Plant Cell 25: 1609-1624
 973 Pastore D, Trono D, Laus MN, Di Fonzo N, Flagella Z (2007) Possible plant mitochondria
 974 involvement in cell adaptation to drought stress: A case study: durum wheat
 975 mitochondria. J. Exp. Bot. 58: 195-210
 976 Peng Z, Lu Q, Verma DPS (1996) Reciprocal regulation of Delta(1)-pyrroline-5-carboxylate
 977 synthetase and proline dehydrogenase genes controls proline levels during and after
 978 osmotic stress in plants. Molec Gen Genet 253: 334-341
 979 Rasmusson AG, Wallstrom SV (2010) Involvement of mitochondria in the control of plant cell
 980 NAD(P)H reduction levels. Bioch Soc Trans 38: 661-666
 981 Roosens NH, Al Bitar F, Loenders K, Angenon G, Jacobs M (2002) Overexpression of ornithine-
 982 delta-aminotransferase increases proline biosynthesis and confers osmotolerance in
 983 transgenic plants. Molec Breed 9: 73-80
 984 Satoh R, Fujita Y, Nakashima K, Shinozaki K, Yamaguchi-Shinozaki KY (2004) A novel
 985 subgroup of bZIP proteins functions as transcriptional activators in hypoosmolarity-
 986 responsive expression of the ProDH gene in Arabidopsis. Plant Cell Physiol 45: 309-317
 987 Satoh R, Nakashima K, Seki M, Shinozaki K, Yamaguchi-Shinozaki K (2002) ACTCAT, a
 988 novel cis-acting element for proline- and hypoosmolarity-responsive expression of the
 989 ProDH gene encoding proline dehydrogenase in Arabidopsis. Plant Physiol 130: 709-719
 990 Sawahel WA, Hassan AH (2002) Generation of transgenic wheat plants producing high levels of
 991 the osmoprotectant proline. Biotechnology Letters 24: 721-725
 992 Schertl P, Cabassa C, Saadallah K, Bordenave M, Savoure A, Braun HP (2014) Biochemical
 993 characterization of proline dehydrogenase in Arabidopsis mitochondria. FEBS J 281:
 994 2794-2804
 995 Schnurr J, Shockey J, Browse J (2004) The Acyl-CoA Synthetase Encoded by LACS2 Is
 996 Essential for Normal Cuticle Development in Arabidopsis. Plant Cell 16: 629-642

997 Senthil-Kumar M, Mysore KS (2012) Ornithine-delta-aminotransferase and proline
 998 dehydrogenase genes play a role in non-host disease resistance by regulating pyrroline-5-
 999 carboxylate metabolism-induced hypersensitive response. *Plant Cell Env* 35: 1329-1343
 1000 Servet C, Ghelis T, Richard L, Zilberstein A, Savoure A (2012) Proline dehydrogenase: a key
 1001 enzyme in controlling cellular homeostasis. *Frontiers in Bioscience-Landmark* 17: 607-
 1002 620
 1003 Sharma S, Verslues PE (2010) Mechanisms independent of ABA or proline feedback have a
 1004 predominant role in transcriptional regulation of proline metabolism during low water
 1005 potential and stress recovery. *Plant Cell Env* 33: 1838-1851
 1006 Sharma S, Villamor JG, Verslues PE (2011) Essential role of tissue-specific proline synthesis
 1007 and catabolism in growth and redox balance at low water potential. *Plant Physiol* 157:
 1008 292-304
 1009 Skirycz A, De Bodt S, Obata T, De Clercq I, Claeys H, De Rycke R, Andriankaja M, Van Aken
 1010 O, Van Breusegem F, Fernie AR, Inze D (2010) Developmental stage specificity and the
 1011 role of mitochondrial metabolism in the response of Arabidopsis leaves to prolonged mild
 1012 osmotic stress. *Plant Physiol.* 152: 226-244
 1013 Su J, Wu R (2004) Stress-inducible synthesis of proline in transgenic rice confers faster growth
 1014 under stress conditions than that with constitutive synthesis. *Plant Sci* 166: 941-948
 1015 Szabados L, Savoure A (2010) Proline: a multifunctional amino acid. *Trends Plant Sci* 15: 89-97
 1016 Szekely G, Abraham E, Csalo A, Rigo G, Zsigmond L, Csiszar J, Ayaydin F, Strizhov N, Jasik J,
 1017 Schmelzer E, Koncz C, Szabados L (2008) Duplicated P5CS genes of Arabidopsis play
 1018 distinct roles in stress regulation and developmental control of proline biosynthesis. *Plant*
 1019 *J* 53: 11-28
 1020 Trenkamp S, Martin W, Tietjen K (2004) Specific and differential inhibition of very-long-chain
 1021 fatty acid elongases from Arabidopsis thaliana by different herbicides. *Proc Natl Acad*
 1022 *Sci USA* 101: 11903-11908
 1023 Verslues PE (2010) Quantification of Water Stress-Induced Osmotic Adjustment and Proline
 1024 Accumulation for *Arabidopsis thaliana* Molecular Genetic Studies. In R Sunkar, ed, *Plant*
 1025 *Stress Tolerance. Methods and Protocols*, Vol Methods in Molecular Biology Vol 639.
 1026 Humana Press, New York, pp 301-316
 1027 Verslues PE, Sharma S (2010) Proline Metabolism and Its Implications for Plant-Environment
 1028 Interaction. *The Arabidopsis Book*: e0140
 1029 Voetberg GS, Sharp RE (1991) Growth of the maize primary root at low water potentials .3.
 1030 Role of increased proline deposition in osmotic adjustment. *Plant Physiol* 96: 1125-1130
 1031 Wang Y, Wu J-F, Nakamichi N, Sakakibara H, Nam H-G, Wu S-H (2011a) LIGHT-
 1032 REGULATED WD1 and PSEUDO-RESPONSE REGULATOR9 form a positive
 1033 feedback regulatory loop in the Arabidopsis circadian clock. *Plant Cell* 23: 486-498
 1034 Wang ZY, Xiong LM, Li WB, Zhu JK, Zhu JH (2011b) The plant cuticle is required for osmotic
 1035 stress regulation of abscisic acid biosynthesis and osmotic stress tolerance in Arabidopsis.
 1036 *Plant Cell* 23: 1971-1984
 1037 Weltmeier F, Ehlert A, Mayer CS, Dietrich K, Wang X, Schutze K, Alonso R, Harter K,
 1038 Vicente-Carbajosa J, Droge-Laser W (2006) Combinatorial control of Arabidopsis
 1039 proline dehydrogenase transcription by specific heterodimerisation of bZIP transcription
 1040 factors. *EMBO J* 25: 3133-3143

1041 Xiao FM, Goodwin SM, Xiao YM, Sun ZY, Baker D, Tang XY, Jenks MA, Zhou JM (2004)
 1042 *Arabidopsis* CYP86A2 represses *Pseudomonas syringae* type III genes and is required for
 1043 cuticle development. *EMBO J* 23: 2903-2913
 1044 Yoshida Y, Kiyosue T, Nakashima K, Yamaguchi-Shinozaki K, Shinozaki K (1997) Regulation
 1045 of levels of proline as an osmolyte in plants under water stress. *Plant Cell Physiol* 38:
 1046 1095-1102
 1047 Zhang CS, Lu Q, Verma DPS (1995) Removal of feedback inhibition of Δ^1 -pyrroline-5-
 1048 carboxylate synthetase, a bifunctional enzyme catalyzing the first 2 steps of proline
 1049 biosynthesis in plants. *J Biol Chem* 270: 20491-20496
 1050 Zhang L, Becker DF (2015) Connecting proline metabolism and signaling pathways in plant
 1051 senescence. *Frontiers in Plant Science* 6 doi.org/10.3389/fpls.2015.00552
 1052 Zhu BC, Su J, Chan MC, Verma DPS, Fan YL, Wu R (1998) Overexpression of a Δ^1 -pyrroline-
 1053 5-carboxylate synthetase gene and analysis of tolerance to water- and salt-stress in
 1054 transgenic rice. *Plant Sci* 139: 41-48
 1055 Zsigmond L, Rigo G, Szarka A, Szekely G, Otvos K, Darula Z, Medzihradszky KF, Koncz C,
 1056 Koncz Z, Szabados L (2008) *Arabidopsis* PPR40 connects abiotic stress responses to
 1057 mitochondrial electron transport. *Plant Physiol.* 146: 1721-1737
 1058
 1059
 1060

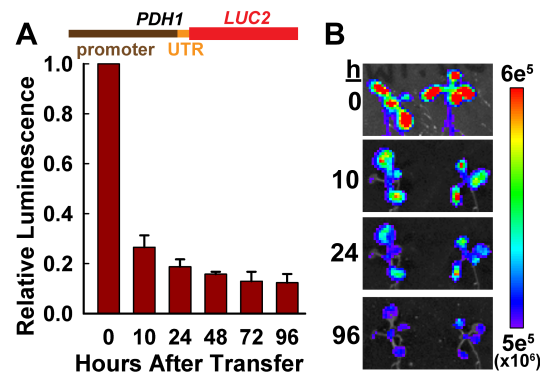


Figure 1: A *PDH1_{pro}::LUC2* reporter responsive to low ψ_w .

- A. The *PDH1* promoter and 5' UTR were fused to the *Luciferase2* (*LUC2*) coding region and used to generate transgenic plants. Quantitation of *PDH1_{pro}::LUC2* luminescence in shoot tissue of seedlings transferred to low ψ_w (-1.0 MPa) for the indicated lengths of time is shown. Data are means \pm S.E. (n=6).
- B. Representative false color images of luminescence intensity from experiments reported in A. Intensity scale for the images is shown at right.

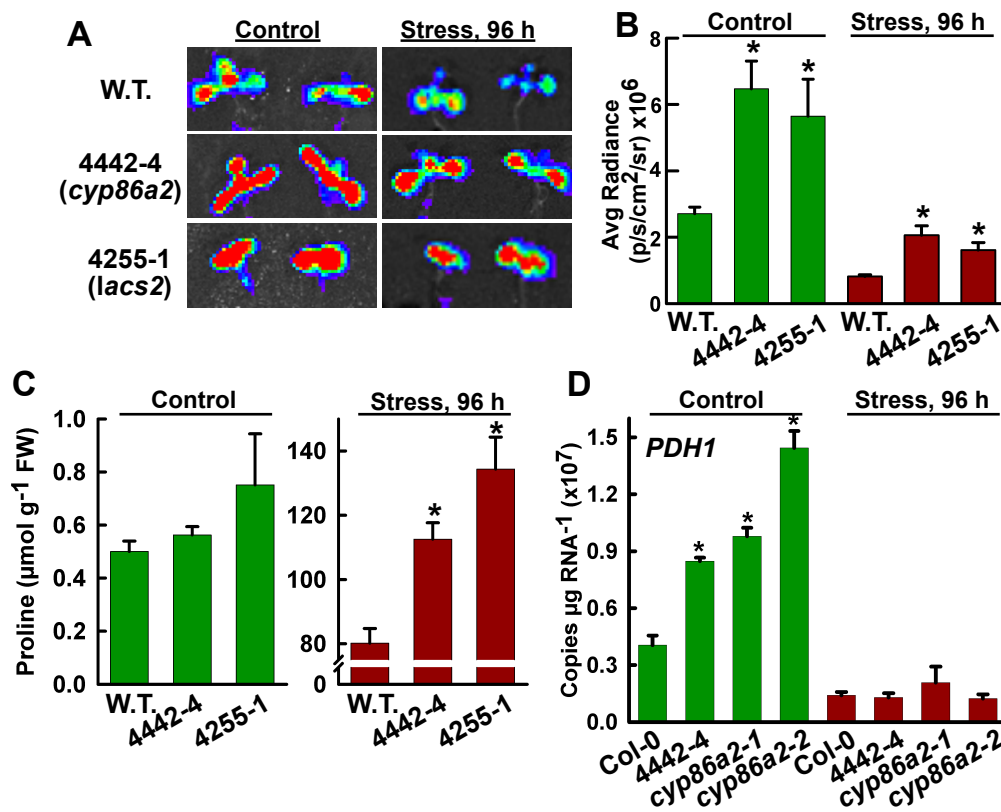


Figure 2: Mutants 4442-4 and 4255-1 have increased *PDH1_{pro}::LUC2* activity and increased proline accumulation at low ψ_w .

- A. Representative false color luminescence images of wild type and mutants in the unstressed control and after 96 h at -1.0 MPa low ψ_w treatment.
- B. Quantification of *PDH1_{pro}::LUC2* activity in 4442-1 and 4255-1. Data are means \pm S.E. (n=4-15). Significant differences ($p \geq 0.05$) compared to wild type in the same treatment are marked (*). Luminescence intensities are given in photons (p) per second (s) per cm² per steradian (sr).
- C. Proline accumulation unstressed control (-0.25 MPa) or low ψ_w stress (-1.2 MPa) for wild type (W.T.) and mutants. Data are means \pm S.E. (n=3-9). Significant differences ($p \geq 0.05$) compared to wild type in the same treatment are marked (*). Note for W.T. is the unmutagenized *PDH1_{pro}::LUC2* line for all experiments in panels A-C.
- D. *PDH1* gene expression in Col-0 wild type, 4442-4 and two T-DNA alleles of *cyp86a2* in the unstressed control treatment or at 96 h after transfer to -1.2 MPa stress. Data are means \pm S.E. (n=3). Significant differences ($p \geq 0.05$) compared to wild type in the same treatment are marked (*). Expression of additional proline metabolism genes in these mutants is shown in Supplemental Figure S4.

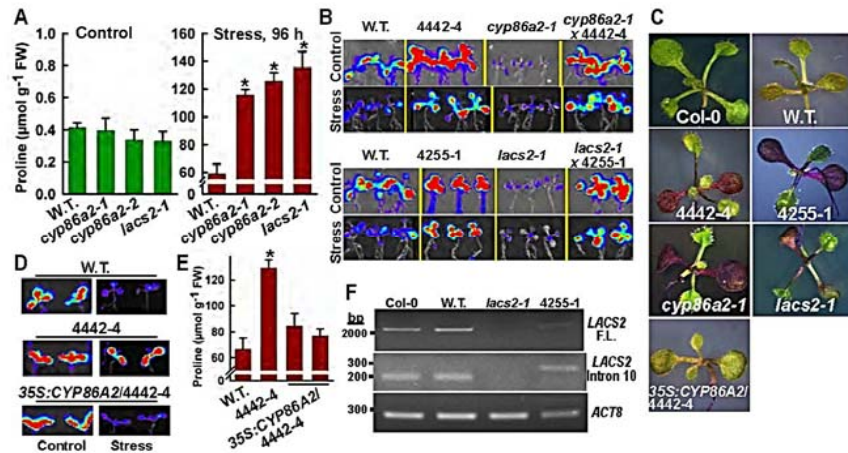


Figure 3: 4442-4 and 4255-1 are alleles of *cyp86a2* and *lacs2*, respectively.

- Proline accumulation in two *cyp86a2* T-DNA alleles and *lacs2-1* under control and -1.2 MPa low ψ_w stress. Data are means ± S.E. (n=4-6) from two experiments. Significant differences (p ≥ 0.05) compared to wild type in the same treatment are marked (*).
- PDHI_{pro}:LUC2* imaging in F₁ seedlings of crosses of 4442-1 and 4255-1 with *cyp86a2-1* and *lacs2-1*, respectively, along with W.T. *PDHI_{pro}:LUC2* and mutant seedlings as controls.
- Toluidine blue staining using seedlings of Col-0, W.T. *PDHI_{pro}:LUC2* as well as mutants and a transgenic complemented line of 4442-4.
- PDHI_{pro}:LUC2* imaging of W.T. *PDHI_{pro}:LUC2*, 4442-4 and 4442-4 complemented with 35S:CYP86A2. Stress treatment was -1.0 MPa for 96 h.
- Stress-induced (-1.2 MPa, 96 h) proline accumulation in 4442-4 and two independent T₃ lines of 4442-4 complemented with 35S:CYP86A2. Data are means ± S.E. (n=4-6) from two experiments. Significant differences (p ≥ 0.05) compared to wild type in the same treatment are marked (*).
- RT-PCR analysis of Col-0, W.T. *PDHI_{pro}:LUC2*, *lacs2-1* and 4255-1 using primers to amplify the full length LACS2 RNA or the region around Intron 10. *ACT8* was used as a reference gene.

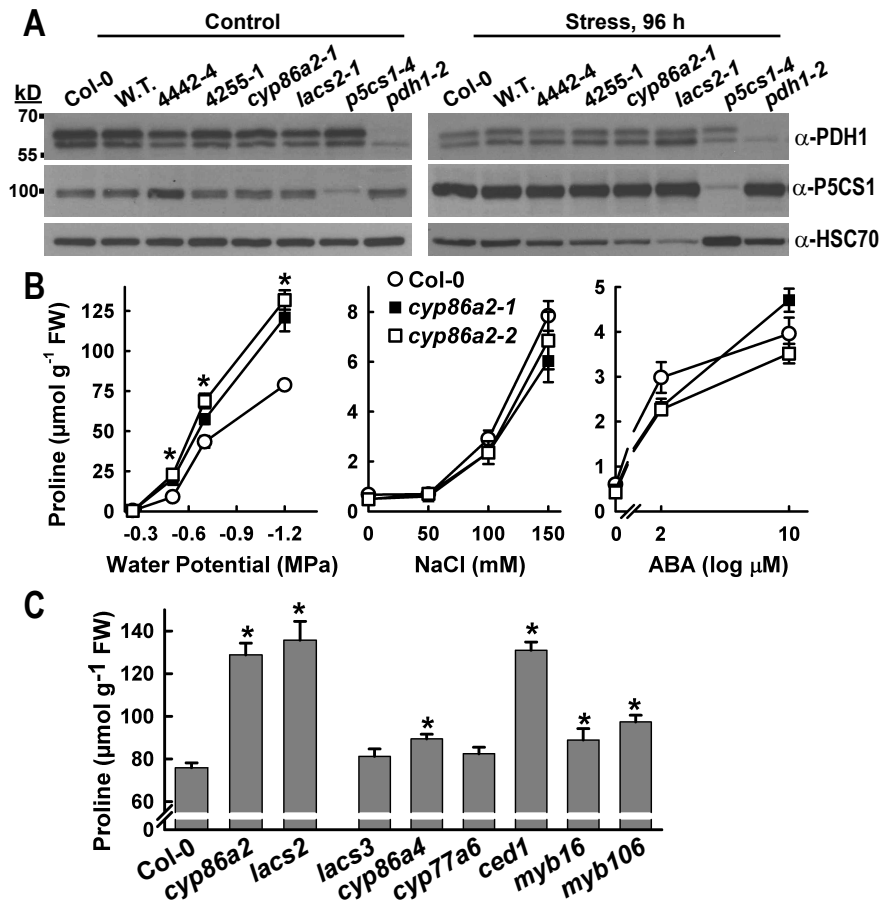


Figure 4: Effects of *cyp86a2* and *lacs2* mutants on proline metabolism and identification of additional cuticle lipid-related mutants with increased proline accumulation at low ψ_w .

- A. Western blot of PDH1 and P5CS1 protein levels in Col-0, W.T. *PDH1_{pro}::LUC2* and *cyp86a2* and *lacs2* mutants. *p5cs1-4* and *pdh1-2* were included to show the specificity of the antisera. Blots were stripped and reprobed with antisera recognizing HSC70 as a loading control. 50 μg of protein was loaded in each lane.
- B. Effect of a range of low ψ_w , salt, or ABA treatments on proline accumulation of Col-0 wild type and *cyp86a2* mutants. Data are means \pm S.E. (n=8-12) from two experiments. Significant differences ($p \geq 0.05$) compared to wild type in the same treatment are marked (*).
- C. Stress-induced (-1.2 MPa, 96 h) proline accumulation in cuticle metabolism mutants. Data are means \pm S.E. (n=11-24) from two experiments. Significant differences ($p \geq 0.05$) compared to wild type are marked (*). For *ced1*, *cyp77a6* and *cyp86a4* the data shown are combined from 2-3 T-DNA alleles which showed identical phenotype. Additional information and RT-PCR verification of T-DNA mutants can be found in Fig S10.

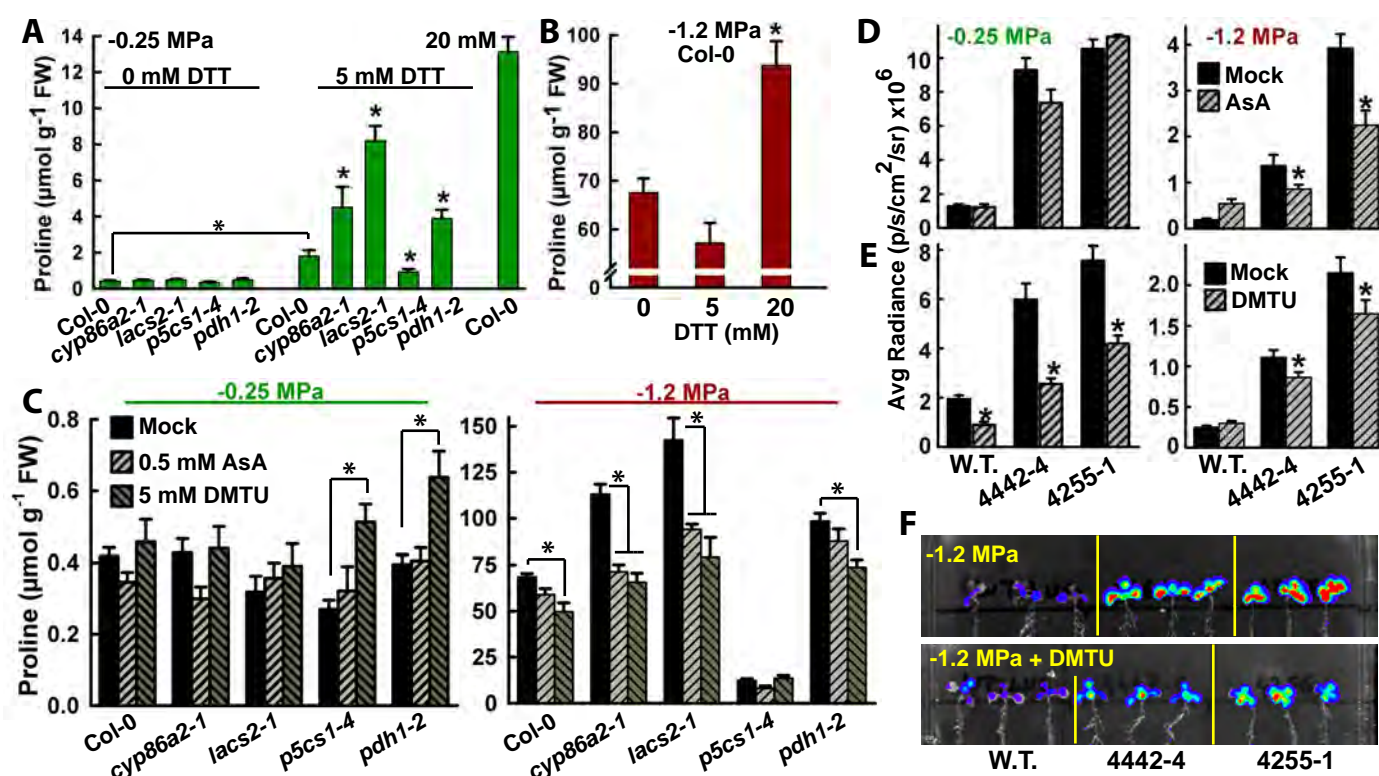


Figure 5: Effect of DTT and reactive oxygen scavengers AsA and DMTU on proline accumulation and *PDH1_{pro}:LUC2* activity.

- A. Effect of DTT treatment on proline accumulation of seedlings at high ψ_w . Data are means \pm S.E. (n=10-44) combined from three experiments. Significant differences ($p \geq 0.05$) compared to wild type in the same treatment or between 0 and 5 mM DTT treatment of wild type are marked (*).
- B. Effect of DTT treatment at -1.2 MPa on proline accumulation. Data are means \pm S.E. (n=10-44) combined from three experiments. Significant differences ($p \geq 0.05$) compared to wild type are marked (*).
- C. Effect of AsA and DMTU on proline levels at -0.25 and -1.2 MPa. Data are means \pm S.E. (n=10-44) combined from three experiments. Significant differences ($p \geq 0.05$) compared to the mock treatment are marked (*).
- D. Effect of AsA on *PDH1_{pro}:LUC2* activity in wild type, 4442-4 and 4255-1 at high (-0.25 MPa) or low ψ_w (-1.2 MPa). Data are means \pm S.E. (n=10-44) combined from three experiments. Significant differences ($p \geq 0.05$) compared to the mock treatment are marked (*).
- E. Effect of DMTU on *PDH1_{pro}:LUC2* activity in wild type, 4442-4 and 4255-1. Data are means \pm S.E. (n=10-44) combined from three experiments. Significant differences ($p \geq 0.05$) compared to the mock treatment are marked (*).
- F. False color imaging of *PDH1_{pro}:LUC2* activity in representative seedlings from the experiments reported in E.

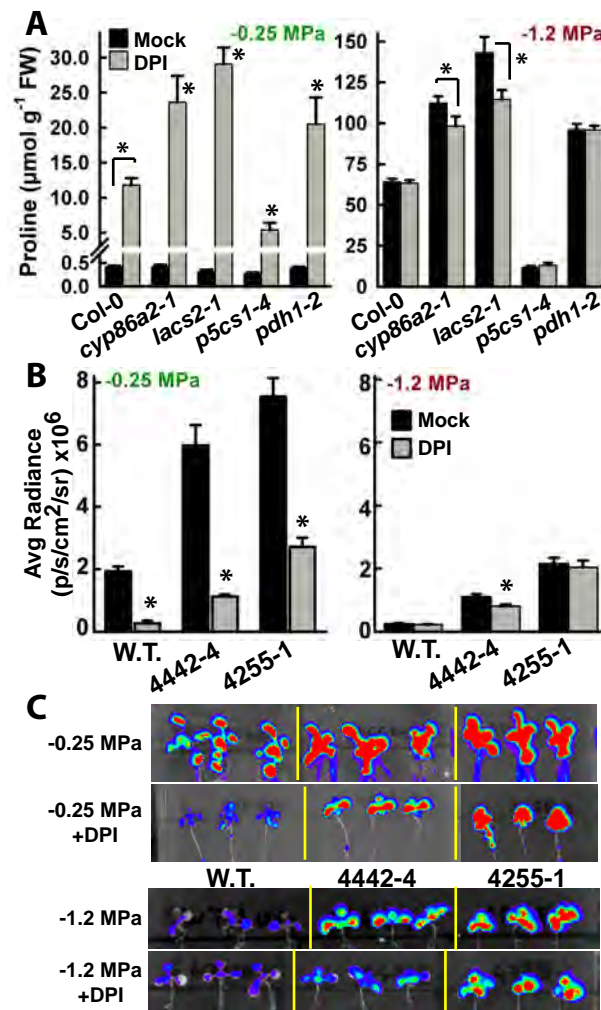


Figure 6: Effect of DPI on proline accumulation and *PDH1_{pro}:LUC2* activity.

- A. Effect of DPI (2.5 μM) on proline accumulation of seedlings at high (-0.25 MPa) or low (-1.2 MPa) ψ_w . Data are means \pm S.E. (n=14-18) combined from three experiments. Significant differences ($p \geq 0.05$) compared to wild type (Col-0) in the same treatment or between mock and DPI treatment of Col-0 are marked (*).
- B. Effect of DPI on *PDH1_{pro}:LUC2* activity in wild type, 4442-4 and 4255-1 at high (-0.25 MPa) or low (-1.2 MPa) ψ_w . Data are means \pm S.E. (n=10-44) combined from three experiments. Significant differences ($p \geq 0.05$) compared to the mock treatment are marked (*).
- C. False color imaging of *PDH1_{pro}:LUC2* activity in representative seedlings from the experiments reported in B.

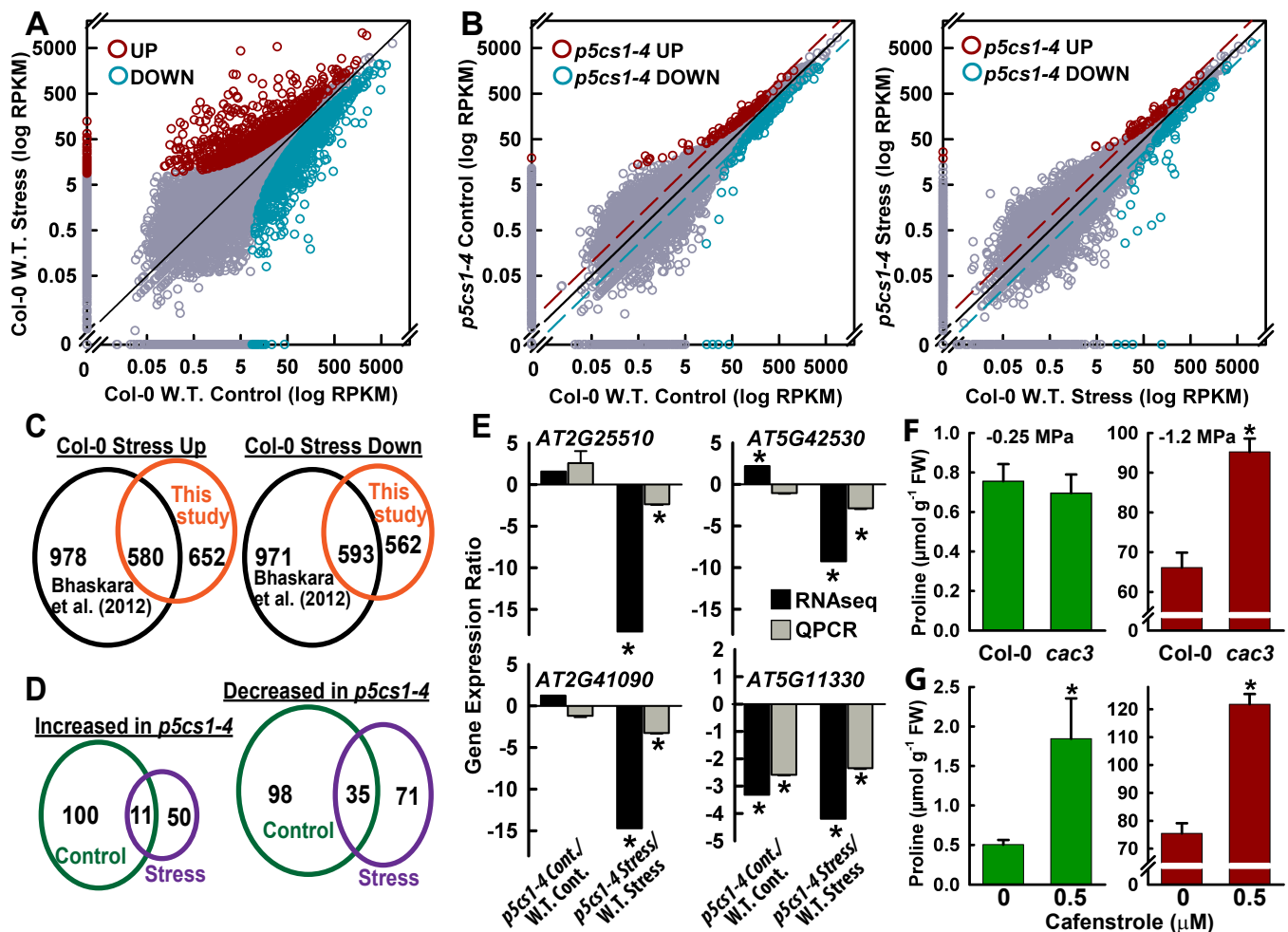


Figure 7: RNA sequencing of Col-0 wild type and *p5cs1-4* shows the effect of proline on chloroplast and mitochondria metabolism and identifies additional lipid metabolism loci affecting proline accumulation.

A. Plot of RPKM values for Col-0 in the unstressed control versus Col-0 after 96 h low ψ_w (-1.2 MPa) treatment. Significantly up- or down-regulated genes are indicated by red or blue circles, respectively while other data points are plotted in grey. Complete listing of RPKM values can be found in Supplemental Table S1 and lists of significantly up or down regulated genes as well as significantly enriched GO terms can be found in Supplemental Tables S2 and S3.

B. Plots of RPKM values for *p5cs1-4* versus Col-0 wild type in the unstressed control treatment and after 96 h low ψ_w treatment. Data presentation is as described for A. Complete listing of RPKM values can be found in Supplemental Table S1 and lists of significantly up or down regulated genes in *p5cs1-4* in both control and stress treatments along with listing of significantly enriched GO terms can be found in Supplemental Tables S4-S7.

C. Comparison of low ψ_w up- or down-regulated genes identified by RNA sequencing to those identified by previous microarray analysis of the same stress treatment.

D. Comparison of genes up- or down regulated in *p5cs1-4* in the control and low ψ_w stress treatment.

E. Comparison of fold change in gene expression detected by RNA sequencing versus fold change detected by QPCR for selected genes down-regulated in *p5cs1-4*. QPCR data are means \pm S.E. (n=5-6) from two experiments. Ratios significant different ($p \geq 0.05$) from 1 based on one sided T-test are indicated.

F. Proline levels in unstressed control (-0.25 MPa) or after 96 h low ψ_w treatment (-1.2 MPa) for Col-0 wild type and *cac3* mutant. Data are means \pm S.E. (n=15-18) from three experiments. Significant difference ($p \geq 0.05$) compared to wild type in the same treatment is marked (*). Effect of the KCS inhibitor cafenstrolo on proline accumulation at high or low ψ_w . Data are means \pm S.E. (n=15-18) from three experiments. Significant differences ($p \geq 0.05$) compared to wild type in the same treatment are marked (*).

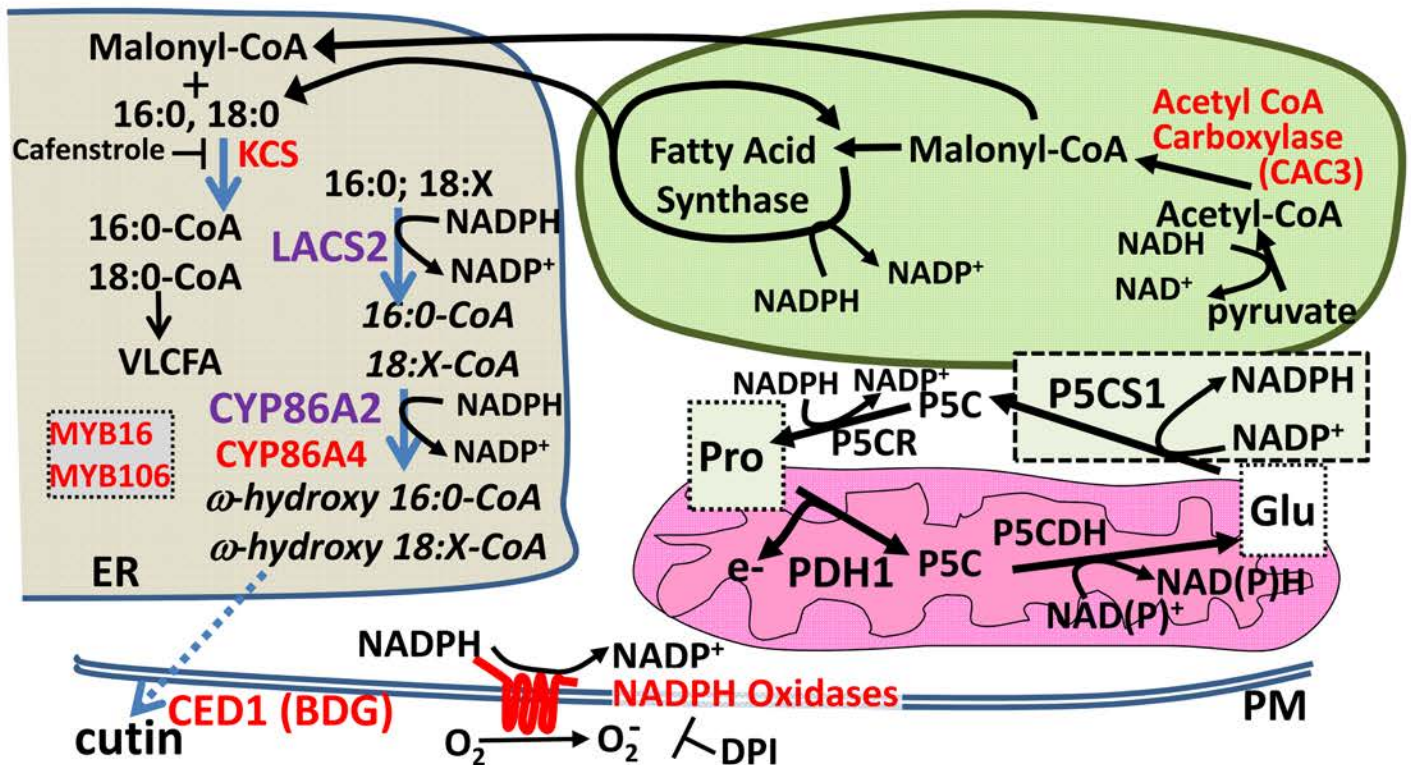


Figure 8: Summary diagram showing the core pathway of proline metabolism in relation to lipid, cuticle and redox-related genes found to affect proline accumulation. Multiple genes and pharmacological treatments disrupting lipid metabolism or NADPH oxidase activity were found to affect proline accumulation and *PDH1_{pro}:LUC2* expression. This included *CYP86A2* and *LACS2* identified in the *PDH1_{pro}:LUC2* forward genetic screen; *CYP86A4*, *CED1*, *MYB16* and *MYB106* identified by reverse genetics; *CAC3* (chloroplast Acetyl CoA Carboxylase complex) and *KCS* genes identified by *p5cs1-4* RNA sequencing as well as strong effects of the NADPH Oxidase inhibitor DPI. The reactions catalyzed by these proteins are spread across several compartments including endoplasmic reticulum (ER), chloroplast and plasma membrane (PM). The commonality among these pathways and proline metabolism itself is an effect on redox status by the consumption of NADPH and regeneration of NADP⁺, either directly as for *P5CS1*, *P5CR*, *LACS2*, *CYP86A2* and NADPH oxidases, or indirectly by modifying the flux through lipid synthesis as for *CAC3*, *KCS*, *CED1*, *MYB16* and *MYB106*. This commonality, along with data obtained with ROS scavengers and DTT treatment, indicates that redox status is a key factor linking these pathways together. Consistent with this, RNA sequencing data showed that *p5cs1-4* had substantial alterations in gene expression related chloroplast and mitochondrial redox metabolism further indicating the relationship of proline to redox status. The similar effects of *p5cs1-4* on gene expression at both high and low ψ_w indicated the importance of proline metabolism, and likely a high rate of flux through the proline cycle of synthesis and catabolism, even in unstressed plants where proline level is low. *P5CS1* is drawn in its own box to indicate that its subcellular localization is unclear. How changes in redox state are communicated between these subcellular compartments is unknown.

Parsed Citations

Abraham E, Rigo G, Szekely G, Nagy R, Koncz C, Szabados L (2003) Light-dependent induction of proline biosynthesis by abscisic acid and salt stress is inhibited by brassinosteroid in Arabidopsis. Plant Molec Biol 51: 363-372

Pubmed: [Author and Title](#)

CrossRef: [Author and Title](#)

Google Scholar: [Author Only](#) [Title Only](#) [Author and Title](#)

Alexa A, Rahnenfuhrer J, Lengauer T (2006) Improved scoring of functional groups from gene

expression data by decorrelating GO graph structure. Bioinformatics 22: 1600-1607

Pubmed: [Author and Title](#)

CrossRef: [Author and Title](#)

Google Scholar: [Author Only](#) [Title Only](#) [Author and Title](#)

Atkin OK, Macherel D (2009) The crucial role of plant mitochondria in orchestrating drought tolerance. Ann Bot 103: 581-597

Pubmed: [Author and Title](#)

CrossRef: [Author and Title](#)

Google Scholar: [Author Only](#) [Title Only](#) [Author and Title](#)

Austin RS, Vidaurre D, Stamatiou G, Breit R, Provart NJ, Bonetta D, Zhang JF, Fung P, Gong YC, Wang PW, McCourt P, Guttman DS (2011) Next-generation mapping of Arabidopsis genes. Plant J 67: 715-725

Pubmed: [Author and Title](#)

CrossRef: [Author and Title](#)

Google Scholar: [Author Only](#) [Title Only](#) [Author and Title](#)

Ben Rejeb K, Abdelly C, Savoure A (2014) How reactive oxygen species and proline face stress together. Plant Physiol Biochem 80: 278-284

Pubmed: [Author and Title](#)

CrossRef: [Author and Title](#)

Google Scholar: [Author Only](#) [Title Only](#) [Author and Title](#)

Ben Rejeb K, Benzarti M, Debez A, Bailly C, Savoure A, Abdelly C (2015) NADPH oxidase-dependent H₂O₂ production is required for salt-induced antioxidant defense in Arabidopsis thaliana. J Plant Physiol 174: 5-15

Pubmed: [Author and Title](#)

CrossRef: [Author and Title](#)

Google Scholar: [Author Only](#) [Title Only](#) [Author and Title](#)

Ben Rejeb K, Lefebvre-De Vos D, Le Disquet I, Leprince AS, Bordenave M, Maldiney R, Jdey A, Abdelly C, Savoure A (2015) Hydrogen peroxide produced by NADPH oxidases increases proline accumulation during salt or mannitol stress in Arabidopsis thaliana. New Phytol 208: 1138-1148

Pubmed: [Author and Title](#)

CrossRef: [Author and Title](#)

Google Scholar: [Author Only](#) [Title Only](#) [Author and Title](#)

Bessire M, Chassot C, Jacquat AC, Humphry M, Borel S, Pet  tot JMC, M  traux JP, Nawrath C (2007) A permeable cuticle in Arabidopsis leads to a strong resistance to Botrytis cinerea. EMBO J 26: 2158-2168

Pubmed: [Author and Title](#)

CrossRef: [Author and Title](#)

Google Scholar: [Author Only](#) [Title Only](#) [Author and Title](#)

Bhaskara GB, Yang TH, Verslues PE (2015) Dynamic proline metabolism: importance and regulation in water limited environments. Frontiers in Plant Sci 6 doi.org/10.3389/fpls.2015.00484

Pubmed: [Author and Title](#)

CrossRef: [Author and Title](#)

Google Scholar: [Author Only](#) [Title Only](#) [Author and Title](#)

Bussis D, Heineke D (1998) Acclimation of potato plants to polyethylene glycol-induced water deficit - II. Contents and subcellular distribution of organic solutes. J Exp Bot 49: 1361-1370

Pubmed: [Author and Title](#)

CrossRef: [Author and Title](#)

Google Scholar: [Author Only](#) [Title Only](#) [Author and Title](#)

Cecchini NM, Monteoliva MI, Alvarez ME (2011) Proline dehydrogenase contributes to pathogen defense in Arabidopsis. Plant Physiol 155: 1947-1959

Pubmed: [Author and Title](#)

CrossRef: [Author and Title](#)

Google Scholar: [Author Only](#) [Title Only](#) [Author and Title](#)

de Ronde JA, Cress WA, Kruger GHJ, Strasser RJ, Van Staden J (2004) Photosynthetic response of transgenic soybean plants, containing an Arabidopsis P5CR gene, during heat and drought stress. J Plant Physiol 161: 1211-1224

Pubmed: [Author and Title](#)

CrossRef: [Author and Title](#)

Google Scholar: [Author Only](#) [Title Only](#) [Author and Title](#)

Dietrich K, Weltmeier F, Ehlert A, Weiste C, Stahl M, Harter K, Droge-Laser W (2011) Heterodimers of the Arabidopsis Transcription Factors bZIP1 and bZIP53 Reprogram Amino Acid Metabolism during Low Energy Stress. Plant Cell 23: 381-395

Pubmed: [Author and Title](#)

CrossRef: [Author and Title](#)

Google Scholar: [Author Only](#) [Title Only](#) [Author and Title](#)

Earley KW, Haag JR, Pontes O, Oppen K, Juehne T, Song KM, Pikaard CS (2006) Gateway-compatible vectors for plant functional genomics and proteomics. *Plant J* 45: 616-629

Pubmed: [Author and Title](#)

CrossRef: [Author and Title](#)

Google Scholar: [Author Only](#) [Title Only](#) [Author and Title](#)

Funck D, Eckard S, Muller G (2010) Non-redundant functions of two proline dehydrogenase isoforms in Arabidopsis. *BMC Plant Biol* 10: 70

Pubmed: [Author and Title](#)

CrossRef: [Author and Title](#)

Google Scholar: [Author Only](#) [Title Only](#) [Author and Title](#)

Funck D, Winter G, Baumgarten L, Forlani G (2012) Requirement of proline synthesis during Arabidopsis reproductive development. *BMC Plant Biol* 12: 1-12

Pubmed: [Author and Title](#)

CrossRef: [Author and Title](#)

Google Scholar: [Author Only](#) [Title Only](#) [Author and Title](#)

Giberti S, Funck D, Forlani G (2014) Delta(1)-pyrroline-5-carboxylate reductase from Arabidopsis thaliana: stimulation or inhibition by chloride ions and feedback regulation by proline depend on whether NADPH or NADH acts as cosubstrate. *New Phytol* 202: 911-919

Pubmed: [Author and Title](#)

CrossRef: [Author and Title](#)

Google Scholar: [Author Only](#) [Title Only](#) [Author and Title](#)

Giraud E, Ho LHM, Clifton R, Carroll A, Estavillo G, Tan Y-F, Howell KA, Ivanova A, Pogson BJ, Millar AH, Whelan J (2008) The Absence of ALTERNATIVE OXIDASE1a in Arabidopsis Results in Acute Sensitivity to Combined Light and Drought Stress. *Plant Physiol.* 147: 595-610

Pubmed: [Author and Title](#)

CrossRef: [Author and Title](#)

Google Scholar: [Author Only](#) [Title Only](#) [Author and Title](#)

Gleeson D, Lelu-Walter MA, Parkinson M (2005) Overproduction of proline in transgenic hybrid larch (*Larix x leptoeuropaea* (Dengler)) cultures renders them tolerant to cold, salt and frost. *Molec Breed* 15: 21-29

Pubmed: [Author and Title](#)

CrossRef: [Author and Title](#)

Google Scholar: [Author Only](#) [Title Only](#) [Author and Title](#)

Hayashi F, Ichino T, Osanai R, Wada K (2000) Oscillation and regulation of proline content by P5CS and ProDH gene expressions in the light/dark cycles in Arabidopsis thaliana L. *Plant Cell Physiol* 41: 1096-1101

Pubmed: [Author and Title](#)

CrossRef: [Author and Title](#)

Google Scholar: [Author Only](#) [Title Only](#) [Author and Title](#)

Kavi Kishor PB, Hima Kumari P, Sunita MSL, Sreenivasulu N (2015) Role of proline in cell wall synthesis and plant development and its implications in plant ontogeny. *Frontiers in Plant Science* 6: doi.org/10.3389/fpls.2015.00544

Pubmed: [Author and Title](#)

CrossRef: [Author and Title](#)

Google Scholar: [Author Only](#) [Title Only](#) [Author and Title](#)

Kent WJ (2002) BLAT - The BLAST-like alignment tool. *Genome Research* 12: 656-664

Pubmed: [Author and Title](#)

CrossRef: [Author and Title](#)

Google Scholar: [Author Only](#) [Title Only](#) [Author and Title](#)

Kesari R, Lasky JR, Villamor JG, Marais DLD, Chen YJC, Liu TW, Lin W, Juenger TE, Verslues PE (2012) Intron-mediated alternative splicing of Arabidopsis P5CS1 and its association with natural variation in proline and climate adaptation. *Proc Natl Acad Sci USA* 109: 9197-9202

Pubmed: [Author and Title](#)

CrossRef: [Author and Title](#)

Google Scholar: [Author Only](#) [Title Only](#) [Author and Title](#)

Kolbe A, Oliver SN, Fernie AR, Stitt M, van Dongen JT, Geigenberger P (2006) Combined transcript and metabolite profiling of Arabidopsis leaves reveals fundamental effects of the thiol-disulfide status on plant metabolism. *Plant Physiol* 141: 412-422

Pubmed: [Author and Title](#)

CrossRef: [Author and Title](#)

Google Scholar: [Author Only](#) [Title Only](#) [Author and Title](#)

Lan P, Li WF, Lin WD, Santi S, Schmidt W (2013) Mapping gene activity of Arabidopsis root hairs. *Genome Biol* 14: R67 DOI: 10.1186/gb-2013-14-6-r67

Pubmed: [Author and Title](#)

CrossRef: [Author and Title](#)

Google Scholar: [Author Only](#) [Title Only](#) [Author and Title](#)

Langmead B, Salzberg SL (2012) Fast gapped-read alignment with Bowtie 2. *Nat Meth* 9: 357-U354

Pubmed: [Author and Title](#)

CrossRef: [Author and Title](#)

Google Scholar: [Author Only](#) [Title Only](#) [Author and Title](#)

Less H, Galili G (2008) Principal Transcriptional Programs Regulating Plant Amino Acid Metabolism in Response to Abiotic

Stresses. Plant Physiol. 147: 316-330

Pubmed: [Author and Title](#)
CrossRef: [Author and Title](#)
Google Scholar: [Author Only](#) [Title Only](#) [Author and Title](#)

Li-Beisson Y, Pollard M, Sauveplane V, Pinot F, Ohlrogge J, Beisson F (2009) Nanoridges that characterize the surface morphology of flowers require the synthesis of cutin polyester. Proc Natl Acad Sci USA 106: 22008-22013

Pubmed: [Author and Title](#)
CrossRef: [Author and Title](#)
Google Scholar: [Author Only](#) [Title Only](#) [Author and Title](#)

Li-Beisson Y, Shorrosh B, Beisson F, Andersson MX, Arondel V, Bates PD, Baud S, Bird D, DeBono A, Durrett TP, Franke RB, Graham IA, Katayama K, Kelly AA, Larson T, Markham JE, Miquel M, Molina I, Nishida I, Rowland O, Samuels L, Schmid KM, Wada H, Welti R, Xu C, Zallot R, Ohlrogge J (2013) Acyl-Lipid Metabolism. The Arabidopsis Book: e0161

Pubmed: [Author and Title](#)
CrossRef: [Author and Title](#)
Google Scholar: [Author Only](#) [Title Only](#) [Author and Title](#)

Liang XW, Zhang L, Natarajan SK, Becker DF (2013) Proline mechanisms of stress survival. Antioxidants & Redox Signaling 19: 998-1011

Pubmed: [Author and Title](#)
CrossRef: [Author and Title](#)
Google Scholar: [Author Only](#) [Title Only](#) [Author and Title](#)

Lin WD, Chen YC, Ho JM, Hsiao CD (2006) GOBU: Toward an integration interface for biological objects. Journal of Information Science and Engineering 22: 19-29

Mattioli R, Biancucci M, Lonoce C, Costantino P, Trovato M (2012) Proline is required for male gametophyte development in Arabidopsis. BMC Plant Biol 12: 1-16

Pubmed: [Author and Title](#)
CrossRef: [Author and Title](#)
Google Scholar: [Author Only](#) [Title Only](#) [Author and Title](#)

Meyer Y, Belin C, Delorme-Hinoux V, Reichheld JP, Riondet C (2012) Thioredoxin and glutaredoxin systems in plants: molecular mechanisms, crosstalks, and functional significance. Antioxidants & Redox Signaling 17: 1124-1160

Pubmed: [Author and Title](#)
CrossRef: [Author and Title](#)
Google Scholar: [Author Only](#) [Title Only](#) [Author and Title](#)

Miller G, Stein H, Honig A, Kapulnik Y, Zilberstein A (2005) Responsive modes of Medicago sativa proline dehydrogenase genes during salt stress and recovery dictate free proline accumulation. Planta 222: 70-79

Pubmed: [Author and Title](#)
CrossRef: [Author and Title](#)
Google Scholar: [Author Only](#) [Title Only](#) [Author and Title](#)

Nakashima K, Satoh R, Kiyosue T, Yamaguchi-Shinozaki K, Shinozaki K (1998) A gene encoding proline dehydrogenase is not only induced by proline and hypoosmolarity, but is also developmentally regulated in the reproductive organs of Arabidopsis. Plant Physiol 118: 1233-1241

Pubmed: [Author and Title](#)
CrossRef: [Author and Title](#)
Google Scholar: [Author Only](#) [Title Only](#) [Author and Title](#)

Nanjo T, Kobayashi M, Yoshida Y, Kakubari Y, Yamaguchi-Shinozaki K, Shinozaki K (1999) Antisense suppression of proline degradation improves tolerance to freezing and salinity in Arabidopsis thaliana. Febs Lett 461: 205-210

Pubmed: [Author and Title](#)
CrossRef: [Author and Title](#)
Google Scholar: [Author Only](#) [Title Only](#) [Author and Title](#)

Nobusawa T, Okushima Y, Nagata N, Kojima M, Sakakibara H, Umeda M (2013) Synthesis of Very-Long-Chain Fatty Acids in the Epidermis Controls Plant Organ Growth by Restricting Cell Proliferation. PLoS Biol 11: e1001531

Pubmed: [Author and Title](#)
CrossRef: [Author and Title](#)
Google Scholar: [Author Only](#) [Title Only](#) [Author and Title](#)

Oshima Y, Shikata M, Koyama T, Ohtsubo N, Mitsuda N, Ohme-Takagi M (2013) MIXTA-Like transcription factors and WAX INDUCER1/SHINE1 coordinately regulate cuticle development in Arabidopsis and Torenia fournieri. Plant Cell 25: 1609-1624

Pubmed: [Author and Title](#)
CrossRef: [Author and Title](#)
Google Scholar: [Author Only](#) [Title Only](#) [Author and Title](#)

Pastore D, Trono D, Laus MN, Di Fonzo N, Flagella Z (2007) Possible plant mitochondria involvement in cell adaptation to drought stress: A case study: durum wheat mitochondria. J. Exp. Bot. 58: 195-210

Pubmed: [Author and Title](#)
CrossRef: [Author and Title](#)
Google Scholar: [Author Only](#) [Title Only](#) [Author and Title](#)

Peng Z, Lu Q, Verma DPS (1996) Reciprocal regulation of Delta(1)-pyrroline-5-carboxylate synthetase and proline dehydrogenase genes controls proline levels during and after osmotic stress in plants. Molec Gen Genet 253: 334-341

Pubmed: [Author and Title](#)

CrossRef: [Author and Title](#)
Google Scholar: [Author Only](#) [Title Only](#) [Author and Title](#)

Rasmusson AG, Wallstrom SV (2010) Involvement of mitochondria in the control of plant cell NAD(P)H reduction levels. Bioch Soc Trans 38: 661-666

Pubmed: [Author and Title](#)
CrossRef: [Author and Title](#)
Google Scholar: [Author Only](#) [Title Only](#) [Author and Title](#)

Roosens NH, Al Bitar F, Loenders K, Angenon G, Jacobs M (2002) Overexpression of ornithine-delta-aminotransferase increases proline biosynthesis and confers osmotolerance in transgenic plants. Molec Breed 9: 73-80

Pubmed: [Author and Title](#)
CrossRef: [Author and Title](#)
Google Scholar: [Author Only](#) [Title Only](#) [Author and Title](#)

Satoh R, Fujita Y, Nakashima K, Shinozaki K, Yamaguchi-Shinozaki KY (2004) A novel subgroup of bZIP proteins functions as transcriptional activators in hypoosmolarity-responsive expression of the ProDH gene in Arabidopsis. Plant Cell Physiol 45: 309-317

Pubmed: [Author and Title](#)
CrossRef: [Author and Title](#)
Google Scholar: [Author Only](#) [Title Only](#) [Author and Title](#)

Satoh R, Nakashima K, Seki M, Shinozaki K, Yamaguchi-Shinozaki K (2002) ACTCAT, a novel cis-acting element for proline- and hypoosmolarity-responsive expression of the ProDH gene encoding proline dehydrogenase in Arabidopsis. Plant Physiol 130: 709-719

Pubmed: [Author and Title](#)
CrossRef: [Author and Title](#)
Google Scholar: [Author Only](#) [Title Only](#) [Author and Title](#)

Sawahel WA, Hassan AH (2002) Generation of transgenic wheat plants producing high levels of the osmoprotectant proline. Biotechnology Letters 24: 721-725

Pubmed: [Author and Title](#)
CrossRef: [Author and Title](#)
Google Scholar: [Author Only](#) [Title Only](#) [Author and Title](#)

Schertl P, Cabassa C, Saadallah K, Bordenave M, Savoure A, Braun HP (2014) Biochemical characterization of proline dehydrogenase in Arabidopsis mitochondria. FEBS J 281: 2794-2804

Pubmed: [Author and Title](#)
CrossRef: [Author and Title](#)
Google Scholar: [Author Only](#) [Title Only](#) [Author and Title](#)

Schnurr J, Shockey J, Browse J (2004) The Acyl-CoA Synthetase Encoded by LACS2 Is Essential for Normal Cuticle Development in Arabidopsis. Plant Cell 16: 629-642

Pubmed: [Author and Title](#)
CrossRef: [Author and Title](#)
Google Scholar: [Author Only](#) [Title Only](#) [Author and Title](#)

Senthil-Kumar M, Mysore KS (2012) Ornithine-delta-aminotransferase and proline dehydrogenase genes play a role in non-host disease resistance by regulating pyrroline-5-carboxylate metabolism-induced hypersensitive response. Plant Cell Env 35: 1329-1343

Pubmed: [Author and Title](#)
CrossRef: [Author and Title](#)
Google Scholar: [Author Only](#) [Title Only](#) [Author and Title](#)

Servet C, Ghelis T, Richard L, Zilberstein A, Savoure A (2012) Proline dehydrogenase: a key enzyme in controlling cellular homeostasis. Frontiers in Bioscience-Landmark 17: 607-620

Pubmed: [Author and Title](#)
CrossRef: [Author and Title](#)
Google Scholar: [Author Only](#) [Title Only](#) [Author and Title](#)

Sharma S, Verslues PE (2010) Mechanisms independent of ABA or proline feedback have a predominant role in transcriptional regulation of proline metabolism during low water potential and stress recovery. Plant Cell Env 33: 1838-1851

Pubmed: [Author and Title](#)
CrossRef: [Author and Title](#)
Google Scholar: [Author Only](#) [Title Only](#) [Author and Title](#)

Sharma S, Villamor JG, Verslues PE (2011) Essential role of tissue-specific proline synthesis and catabolism in growth and redox balance at low water potential. Plant Physiol 157: 292-304

Pubmed: [Author and Title](#)
CrossRef: [Author and Title](#)
Google Scholar: [Author Only](#) [Title Only](#) [Author and Title](#)

Skirycz A, De Bodt S, Obata T, De Clercq I, Claeys H, De Rycke R, Andriankaja M, Van Aken O, Van Breusegem F, Fernie AR, Inze D (2010) Developmental stage specificity and the role of mitochondrial metabolism in the response of Arabidopsis leaves to prolonged mild osmotic stress. Plant Physiol. 152: 226-244

Pubmed: [Author and Title](#)
CrossRef: [Author and Title](#)
Google Scholar: [Author Only](#) [Title Only](#) [Author and Title](#)

Su J, Wu R (2004) Stress-inducible synthesis of proline in transgenic rice confers faster growth under stress conditions than that

with constitutive synthesis. Plant Sci 166: 941-948

Pubmed: [Author and Title](#)

CrossRef: [Author and Title](#)

Google Scholar: [Author Only](#) [Title Only](#) [Author and Title](#)

Szabados L, Savoure A (2010) Proline: a multifunctional amino acid. Trends Plant Sci 15: 89-97

Pubmed: [Author and Title](#)

CrossRef: [Author and Title](#)

Google Scholar: [Author Only](#) [Title Only](#) [Author and Title](#)

Szekely G, Abraham E, Csalo A, Rigo G, Zsigmond L, Csiszar J, Ayaydin F, Strizhov N, Jasik J, Schmelzer E, Koncz C, Szabados L (2008) Duplicated P5CS genes of Arabidopsis play distinct roles in stress regulation and developmental control of proline biosynthesis. Plant J 53: 11-28

Pubmed: [Author and Title](#)

CrossRef: [Author and Title](#)

Google Scholar: [Author Only](#) [Title Only](#) [Author and Title](#)

Trenkamp S, Martin W, Tietjen K (2004) Specific and differential inhibition of very-long-chain fatty acid elongases from Arabidopsis thaliana by different herbicides. Proc Natl Acad Sci USA 101: 11903-11908

Pubmed: [Author and Title](#)

CrossRef: [Author and Title](#)

Google Scholar: [Author Only](#) [Title Only](#) [Author and Title](#)

Verslues PE (2010) Quantification of Water Stress-Induced Osmotic Adjustment and Proline Accumulation for Arabidopsis thaliana Molecular Genetic Studies. In R Sunkar, ed, Plant Stress Tolerance. Methods and Protocols, Vol Methods in Molecular Biology Vol 639. Humana Press, New York, pp 301-316

Pubmed: [Author and Title](#)

CrossRef: [Author and Title](#)

Google Scholar: [Author Only](#) [Title Only](#) [Author and Title](#)

Verslues PE, Sharma S (2010) Proline Metabolism and Its Implications for Plant-Environment Interaction. The Arabidopsis Book: e0140

Pubmed: [Author and Title](#)

CrossRef: [Author and Title](#)

Google Scholar: [Author Only](#) [Title Only](#) [Author and Title](#)

Voetberg GS, Sharp RE (1991) Growth of the maize primary root at low water potentials .3. Role of increased proline deposition in osmotic adjustment. Plant Physiol 96: 1125-1130

Pubmed: [Author and Title](#)

CrossRef: [Author and Title](#)

Google Scholar: [Author Only](#) [Title Only](#) [Author and Title](#)

Wang Y, Wu J-F, Nakamichi N, Sakakibara H, Nam H-G, Wu S-H (2011a) LIGHT-REGULATED WD1 and PSEUDO-RESPONSE REGULATOR9 form a positive feedback regulatory loop in the Arabidopsis circadian clock. Plant Cell 23: 486-498

Pubmed: [Author and Title](#)

CrossRef: [Author and Title](#)

Google Scholar: [Author Only](#) [Title Only](#) [Author and Title](#)

Wang ZY, Xiong LM, Li WB, Zhu JK, Zhu JH (2011b) The plant cuticle is required for osmotic stress regulation of abscisic acid biosynthesis and osmotic stress tolerance in Arabidopsis. Plant Cell 23: 1971-1984

Pubmed: [Author and Title](#)

CrossRef: [Author and Title](#)

Google Scholar: [Author Only](#) [Title Only](#) [Author and Title](#)

Weltmeier F, Ehlert A, Mayer CS, Dietrich K, Wang X, Schutze K, Alonso R, Harter K, Vicente-Carbajosa J, Droge-Laser W (2006) Combinatorial control of Arabidopsis proline dehydrogenase transcription by specific heterodimerisation of bZIP transcription factors. EMBO J 25: 3133-3143

Pubmed: [Author and Title](#)

CrossRef: [Author and Title](#)

Google Scholar: [Author Only](#) [Title Only](#) [Author and Title](#)

Xiao FM, Goodwin SM, Xiao YM, Sun ZY, Baker D, Tang XY, Jenks MA, Zhou JM (2004) Arabidopsis CYP86A2 represses Pseudomonas syringae type III genes and is required for cuticle development. EMBO J 23: 2903-2913

Pubmed: [Author and Title](#)

CrossRef: [Author and Title](#)

Google Scholar: [Author Only](#) [Title Only](#) [Author and Title](#)

Yoshida Y, Kiyosue T, Nakashima K, Yamaguchi-Shinozaki K, Shinozaki K (1997) Regulation of levels of proline as an osmolyte in plants under water stress. Plant Cell Physiol 38: 1095-1102

Pubmed: [Author and Title](#)

CrossRef: [Author and Title](#)

Google Scholar: [Author Only](#) [Title Only](#) [Author and Title](#)

Zhang CS, Lu Q, Verma DPS (1995) Removal of feedback inhibition of γ -pyrroline-5-carboxylate synthetase, a bifunctional enzyme catalyzing the first 2 steps of proline biosynthesis in plants. J Biol Chem 270: 20491-20496

Pubmed: [Author and Title](#)

CrossRef: [Author and Title](#)

Google Scholar: [Author Only](#) [Title Only](#) [Author and Title](#)

Zhang L, Becker DF (2015) Connecting proline metabolism and signaling pathways in plant senescence. Frontiers in Plant Science

6 doi.org/10.3389/fpls.2015.00552

Pubmed: [Author and Title](#)

CrossRef: [Author and Title](#)

Google Scholar: [Author Only](#) [Title Only](#) [Author and Title](#)

Zhu BC, Su J, Chan MC, Verma DPS, Fan YL, Wu R (1998) Overexpression of a γ -pyrroline-5-carboxylate synthetase gene and analysis of tolerance to water- and salt-stress in transgenic rice. Plant Sci 139: 41-48

Pubmed: [Author and Title](#)

CrossRef: [Author and Title](#)

Google Scholar: [Author Only](#) [Title Only](#) [Author and Title](#)

Zsigmond L, Rigo G, Szarka A, Szekely G, Otvos K, Darula Z, Medzihradszky KF, Koncz C, Koncz Z, Szabados L (2008) Arabidopsis PPR40 connects abiotic stress responses to mitochondrial electron transport. Plant Physiol. 146: 1721-1737

Pubmed: [Author and Title](#)

CrossRef: [Author and Title](#)

Google Scholar: [Author Only](#) [Title Only](#) [Author and Title](#)